Open access • Journal Article • DOI:10.1007/S00291-003-0125-7

Intensity-modulated radiotherapy – a large scale multi-criteria programming problem — Source link

Karl-Heinz Küfer, Alexander Scherrer, Michael Monz, Fernando Alonso ...+3 more authors

Institutions: Daimler AG, Harvard University, German Cancer Research Center

Published on: 01 May 2003 - OR Spectrum (Springer-Verlag)

Topics: Pareto principle, Evaluation function and Linear programming

Fraunhofer Institut
Techno- und
Wirtschaftsmathematik

T. Bortfeld , K.-H. Küfer, M. Monz, A. Scherrer,
C. Thieke, H. Trinkaus

Intensity-Modulated Radiotherapy: A Large Scale Multi-Criteria Programming Problem

Berichte des Fraunhofer ITWM, Nr. 43 (2003)

ISSN 1434-9973

Bericht 43 (2003)

Die Veröffentlichungen in der Berichtsreihe des Fraunhofer ITWM können bezogen werden über:

Fraunhofer-Institut für Techno- und
Wirtschaftsmathematik ITWM
Gottlieb-Daimler-Straße, Geb. 49

67663 Kaiserslautern

Telefon: +49 (0) 6 31/2 05-32 42
Telefax: +49 (0) 6 31/2 05-41 39
E-Mail: info@itwm.fraunhofer.de
Internet: www.itwm.fraunhofer.de

Vorwort

Das Tätigkeitsfeld des Fraunhofer Instituts für Techno- und Wirtschaftsmathematik ITWM umfasst anwendungsnahe Grundlagenforschung, angewandte Forschung sowie Beratung und kundenspezifische Lösungen auf allen Gebieten, die für Techno- und Wirtschaftsmathematik bedeutsam sind.

In der Reihe »Berichte des Fraunhofer ITWM« soll die Arbeit des Instituts kontinuierlich einer interessierten Öffentlichkeit in Industrie, Wirtschaft und Wissenschaft vorgestellt werden. Durch die enge Verzahnung mit dem Fachbereich Mathematik der Universität Kaiserslautern sowie durch zahlreiche Kooperationen mit internationalen Institutionen und Hochschulen in den Bereichen Ausbildung und Forschung ist ein großes Potenzial für Forschungsberichte vorhanden. In die Berichtreihe sollen sowohl hervorragende Diplom- und Projektarbeiten und Dissertationen als auch Forschungsberichte der Institutsmitarbeiter und Institutsgäste zu aktuellen Fragen der Techno- und Wirtschaftsmathematik aufgenommen werden.

Darüberhinaus bietet die Reihe ein Forum für die Berichterstattung über die zahlreichen Kooperationsprojekte des Instituts mit Partnern aus Industrie und Wirtschaft.

Berichterstattung heißt hier Dokumentation darüber, wie aktuelle Ergebnisse aus mathematischer Forschungs- und Entwicklungsarbeit in industrielle Anwendungen und Softwareprodukte transferiert werden, und wie umgekehrt Probleme der Praxis neue interessante mathematische Fragestellungen generieren.

Prof. Dr. Dieter Prätzel-Wolters
Institutsleiter

Kaiserslautern, im Juni 2001

Intensity-Modulated Radiotherapy - A Large Scale Multi-Criteria Programming Problem -

Thomas Bortfeld
Department of Radiation Oncology
Massachusetts General Hospital
and Harvard Medical School
Boston, USA

Christian Thieke
Department of Medical Physics
German Cancer Research Center
Heidelberg, Germany

Karl-Heinz Küfer, Michael Monz,
Alexander Scherrer, Hans Trinkaus
Department of Optimization
Fraunhofer Institut for Industrial Mathematics
Kaiserslautern, Germany

December 17, 2002

Summary: Radiation therapy planning is always a tight rope walk between dangerous insufficient dose in the target volume and life threatening overdosing of organs at risk. Finding ideal balances between these inherently contradictory goals challenges dosimetrists and physicians in their daily practice. Todays planning systems are typically based on a single evaluation function that measures the quality of a radiation treatment plan. Unfortunately, such a one dimensional approach cannot satisfactorily map the different backgrounds of physicians and the patient dependent necessities. So, too often a time consuming iteration process between evaluation of dose distribution and redefinition of the evaluation function is needed.
In this paper we propose a generic multi-criteria approach based on Pareto's solution concept. For each entity of interest - target volume or organ at risk a structure dependent evaluation function is defined measuring deviations from ideal doses that are calculated from statistical functions. A reasonable bunch of clinically meaningful Pareto optimal solutions are stored in a data base, which can be interactively searched by physicians. The system guarantees dynamical planning as well as the discussion of tradeoffs between different entities.
Mathematically, we model the upcoming inverse problem as a multi-criteria

linear programming problem. Because of the large scale nature of the problem it is not possible to solve the problem in a 3D-setting without adaptive reduction by appropriate approximation schemes.
Our approach is twofold: First, the discretization of the continuous problem is based on an adaptive hierarchical clustering process which is used for a local refinement of constraints during the optimization procedure. Second, the set of Pareto optimal solutions is approximated by an adaptive grid of representatives that are found by a hybrid process of calculating extreme compromises and interpolation methods.

Keywords: multiple criteria optimization, representative systems of Pareto solutions, adaptive triangulation, clustering and disaggregation techniques, visualization of Pareto solutions, medical physics, external beam radiotherapy planning, intensity modulated radiotherapy

1 Introduction

Intensity-modulated radiotherapy (IMRT) has a much greater potential to shape dose distributions than conventional radiotherapy with uniform beams [2]. This capability has been used to tailor the dose distribution to the tumor target volume in conformal radiotherapy. In general IMRT allows one to achieve a better dose conformation, especially for irregularly shaped concave target volumes. The improved physical characteristics of IMRT can lead to improved clinical results, as was suggested in recent clinical studies. Although IMRT is already in clinical use at several hospitals in Europe and many in the USA, there is a lot of potential and need for further improvements.
In most systems IMRT planning is considered as an optimization problem. The goal is to find the parameters (intensity maps, sometimes also beam orientations, energy, etc.) that yield the best possible treatment plan under consideration of various clinical, technical, and physical constraints. A huge number of current research activities is related to this problem. In this presentation we will focus on the principal optimization concept.

1.1 Current optimization strategies

IMRT allows for a much greater flexibility in the delivery of spatial radiation dose distributions. Nevertheless, because of physical limitations, it cannot deliver the ideal dose distribution, which is 100% in the target volume and 0% everywhere else. While IMRT does allow to achieve a somewhat steeper dose gradient between normal tissue and the target volume, especially for irregularly shaped targets, the steepness of the gradients is still physically limited; the 20% to 80% penumbra is at least about 6 mm wide. As a consequence of this, if the target is directly abutting to a critical structure,

the minimum target dose equals the maximal dose in the critical structure. In a more general sense, the goals of delivering a high dose to the target and a small dose to the critical structures contradict each other.

1. Weight factors
   A realistic objective can only be to find a suitable compromise between target coverage and normal tissue sparing. One way how this is actually done in current IMRT planning systems is to combine objectives or costlets for the different critical structures (FR) and the target volume (FT) using weight factors w (also called penalties or importance factors). Mathematically, an objective function is defined that is of the form $F = w_T F_T + w_1 F_{R_1} + \ldots + w_K F_{R_K}$. By using a large value for w_T, more emphasize is put on the target dose, and vice versa. The problem of this approach is that the weight factors have no clinical meaning. Suitable weight factors have to be determined by trial and error, which may be quite time consuming.

2. Constraints
   Another approach, which is also used in commercial planning systems, uses constraints on, say, the maximum dose in the critical structures or the minimum dose in the target. Here the potential problem is that there is no reward for reducing the dose in the critical structures below the tolerance.

A problem with both of the above approaches (weighting and constraining) is that in general there is no "sensitivity analysis" done. That means, it is unclear how dependent the dose in one structure, say the target, is on the constraints in other structures.

1.2 The new optimization paradigm - a generic multi-criteria concept

To solve the above-mentioned drawbacks and problems in IMRT planning, a new optimization concept was developed in collaboration between the Fraunhofer Institute for Industrial Mathematics (ITWM), Kaiserslautern, Germany, German Cancer Research Center (DKFZ), Heidelberg, Germany, and Massachusetts General Hospital (MGH), Boston (MA), United States. Instead of defining a single objective function as a measure of the quality of the treatment plan, the new approach is generically multi-criteria. To characterize the dose distribution in each structure (critical structures and target), we use the equivalent uniform dose (EUD) [9]. This is defined as the uniform dose that leads to the same effect as the actual non-uniform dose in that organ. The whole plan is characterized by the set of EUDs in the

different organs. What we seek is an optimal compromise between the EUDs in the target and the critical structures. Now, there is an infinite number of combinations of those EUD values. To make the search tractable, we look at so-called efficient (Pareto optimal) solutions only [13]. These are defined as combinations of EUDs in which an improvement of the EUD in one organ will always lead to a worse result in at least one of the other organs. The advantages of this concept are threefold:

1. Artificial weight factors, which have no clinical meaning, are avoided. The whole concept is based on dose-like values, which are amenable to a clinical interpretation.

2. Unnecessarily high doses in some of the critical structures, which can occur in constrained optimization (see above), are avoided by definition of the efficient (Pareto) solution.

3. Plan tuning can be done interactively using "knobs" that have a clinical meaning. It is easy to do a sensitivity analysis and determine the dependency of, say, the target EUD on any of the critical structure EUDs.

The last point requires further explanation. The new concept comprises a database in which a large number of efficient solutions are stored. The solutions are calculated and the database is filled over night. At the planning stage, the treatment planner and the physician can search the database interactively. At the beginning, the system suggests a balanced solution that matches the planning goals to a large degree. If one or more aspects of the plan are not desirable (e.g., the EUD in one critical structure is too high), the planner can immediately go to another solution in which that specific criterion is fulfilled. In this way the relevant solutions can be explored interactively and the most suitable solution can be found efficiently.

2 The mathematical model

Throughout the rest of the paper we will assume that a meaningful *irradiation geometry*, i.e. the number and the directions of beams are given. Typically but not necessarily in case of IMRT, the irradiation geometry will be isocentric and coplanary. The absorbed dose $d = d(\xi)$ in an infinitesimally small element $v \in V$ of the relevant body volume V is given by the formula

$$d(\xi)(v) = \int_B p(v,b)\xi(b)db \tag{1}$$

where ξ is the fluence distribution on the beamheads B. $p(v,b)$ represents the dose deposit in $v \in V$ from the infinitesimal beam element $b \in B$ under

unit fluence. We assume in this paper, that p is given in an appropriate way. Evaluation of radiation therapy plans is done by discussing the dose distribution $d|_{V_k}$, $k \in \{T, R_1, R_2, \ldots, R_K\}$ for all entities of interest, i.e. target and risk structures separately. The goal of a radiation therapy treatment planning is to determine the fluence distribution $\xi \geq 0$ in such a way that the dose distribution in any entity of interest approximately satisfies some ideal bounds, which guarantee a high of*t*umor control probability (TCP) and a low *n*ormal tissue complication probability (NTCP).

2.1 The equivalent uniform dose - EUD

TCP and NTCP functions can be mathematically described using the *equivalent uniform dose* (EUD) model. Here, a non-uniform dose distribution $d|_{V_k}$ is related to a uniform dose level $\mathrm{EUD}_k(d)$ that generates a comparable biological impact. In literature there are some approaches for modelling the EUD based on statistical data. E.g. Niemierko [12] defines EUDs with the aid of normalized q-norms, i.e. $\mathrm{EUD}_k(d) = \|d\|_{q,k}$, where q is organ dependent and found by curve fitting methods from statistical complication probabilities, cf. [8]. For critical structures q ranges between 1 and ∞. If an organ is more parallely organized like e.g. the lung, q will be close to 1, i.e. the EUD will be close to the mean dose. If on the other hand, an organ is more serially organized like the spinal chord, q will be close to ∞, i.e. the EUD will be close to the maximum dose. A similar concept is due to Thieke, Bortfeld, and Küfer [14], who defined the EUD by convex combinations of the mean dose and the maximum dose, i.e. depending on the organisational structure of the organ

$$\mathrm{EUD}_k(d) = \alpha_k \cdot d^{max(k)} + (1 - \alpha_k) \cdot d^{mean(k)} \tag{2}$$

for an appropriate organ dependent $\alpha_k \in [0, 1]$. Analogously to Niemierko's q-scale, α_k will be close to 1 for more serial organs, while α_k will be close to 1 for more parallel organs. A table with values for organ related q's and α's based on statistical data by Burman, Kutcher, Emami and Gotein can be found in [3]. Notice, that for both EUD-models the function EUD_k is homogeneous, i.e. $\mathrm{EUD}_k(\lambda d) = \lambda \mathrm{EUD}_k(d)$ for $\lambda \geq 0$. This property aside the convexity of the EUD_k-functions will be important for the optimization approach described in Section 3.
The biological impact of the absorbed dose in the target can be described by the minimal dose value.
In terms of the EUD, the NTCP (normal tissue complication probability) functions of the different organs at risk $R_1, \ldots, R_K$ are S-shaped functions, while the TCP (tumor control probability) is an S-shaped function defined on the minimum dose value in the target, cf. Figure (1).

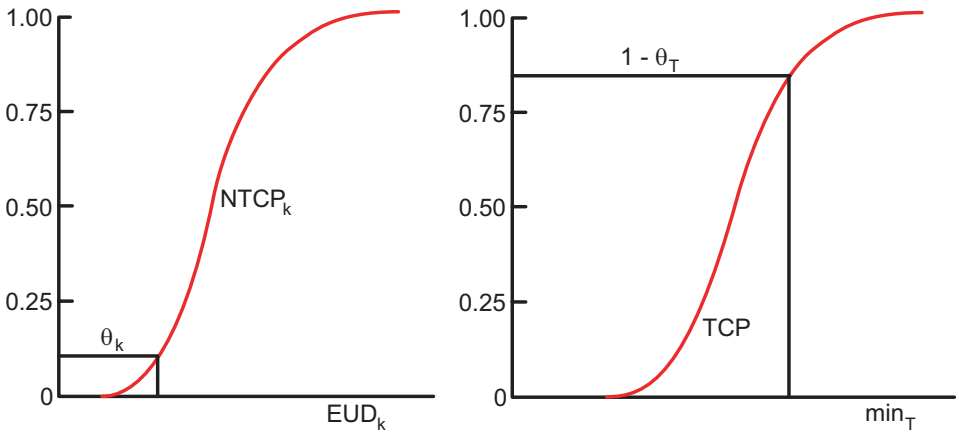

Figure 1: The S-shaped NTCP- and TCP- functions

An ideal dose distribution function d would meet the following conditions

$$\begin{aligned} \mathrm{NTCP}_k(\mathrm{EUD}_k(d(\xi)) &\leq \theta_k, \quad k \in \{R_1, \ldots, R_K\} \\ \mathrm{TCP}(\min_T(d(\xi))) &\geq 1 - \theta_T \end{aligned} \tag{3}$$

where typically all θ_k will lie below some thresholds $\leq 5\%$. If we rewrite this condition by inverting the S-shaped functions, this leads to a system of inequalities of type

$$\begin{aligned} \mathrm{EUD}_k(d(\xi)) &\leq U_k, \quad k \in \{R_1, \ldots, R_K\} \\ \min_T(d(\xi)) &\geq L \end{aligned} \tag{4}$$

where $U_k = \mathrm{NTCP}_k^{-1}(\theta_k)$ for $k \in \{R_1, \ldots, R_K\}$ and $L = \mathrm{TCP}^{-1}(1 - \theta_T)$. Unfortunately, the inequality system (4) will in general be mathematically infeasible due to the physical constraint $\xi \geq 0$. Hence, the problem is to calculate a fluence distribution that results in a tight approximation of (4). In the language of therapists this means we have to find a decent compromise between overdosing of the risks and underdosing of the target in the light of the ideal dose bounds U_k and L.

2.2 Multi-criteria optimization of radiotherapy - definition of a planning domain

Deviations from the ideal goals (4) can be represented by use of costlet functions F_k, that define relative deviations from the ideal goals. More precisely,

$$\begin{aligned} F_k(\xi) &= \frac{\mathrm{EUD}_k(d(\xi)) - U_k}{U_k}, \quad k \in \{R_1, \ldots, R_K\}, \\ F_T(\xi) &= \frac{L - \min_T(d(\xi))}{L} \end{aligned} \tag{5}$$

The radiation therapy planning problem can now be expressed as the following multi-criteria optimization problem

$$\begin{aligned} F_k(\xi) &\rightarrow \text{Min}, \ k \in \{T, R_1, \ldots, R_K\} \quad \text{subject to} \\ \xi &\geq 0 \end{aligned} \tag{6}$$

Problem (6) is a restricted convex optimization problem, if the EUD-functions are convex in ξ. This is true for Niemiercko's q-scale concept and for the max-and-mean model from (2) as well.
Up to now, in the radiation therapy planning community problem (6) is solved by a weighted scalarized approach: Define positive weights w_k solve the optimization problem

$$\begin{aligned} F_w(\xi) = \sum_{k \in \{T, R_1, \ldots, R_K\}} w_k F_k(\xi) &\rightarrow \text{Min} \quad \text{subject to} \\ \xi &\geq 0, \end{aligned}$$

check the quality by eye using appropriate dose visualizations and update w_k by trial and error until a satisfactory result is achieved. This process is time consuming and does not allow dynamical treatment planning, cf. Bortfeld [7]. Therefore, Hamacher und Küfer proposed in [5] a generic multi-criteria approach, that is based on Pareto-optimal solutions. A fluence distribution ξ is called efficient or Pareto-optimal for (6), if there is no additional improvement for one of the costlets F_k without worsening at least one of the others.
Unfortunately, the class of Pareto solutions also includes "bad compromises" that are clinically irrelevant. E.g. a zero fluence is Pareto-optimal, since an improvement in the target would require to worsen at least one of the risks. Hence there is need to define a planning domain that covers only clinically meaningful solutions and approximates relevant parts of the set of Pareto-optimal solutions.
This is done with the aid of an equibalanced solution, defined by:

$$\begin{aligned} s &\rightarrow \text{Min} \quad \text{subject to} \\ F_k(\xi) &\leq s, \qquad k \in \{T, R_1, \ldots, R_K\}, \\ \xi &\geq 0. \end{aligned} \tag{7}$$

Problem (7) always gives a *least common tolerance* value s^* that will hold for all relative deviations F_k. A solution ξ of (7) can be seen as a prototype of a balanced solution that will lead in the clinical meaningful area. Though a solution of (7) guarantees mathematically a balance between the planning goals in (6), it is absolutely necessary for planning purposes to have a platform for further plan tuning, as the evaluation functionals F_k cannot reflect the dose distribution completely.

For this reason, we define the *planning domain* as a neighborhood of an equibalanced solution defined by (7) with

$$\begin{aligned} \mathrm{PD}(S) := \{\xi \geq 0 : \quad & F_k(\xi) && \leq s_k,\ k = T, R_1, \ldots R_k\} \\ = \{\xi \geq 0 : \quad & \mathrm{EUD}_k(d(\xi)) && \leq U_k(1 + s_k),\ k = R_1, \ldots R_k, \\ & \min_T d(\xi) && \geq L(1 - s_T)\}, \end{aligned} \tag{8}$$

where $S := (s_k)$ denotes the vector with the entries $s_k := s^* + \Delta s_k$, $k \in \{T, R_1, \ldots, R_K\}$ with $\Delta s_k > 0$. Typically, the values of Δs_k should be chosen such that known hard constraints from statistical data on tumor control probabilities and normal tissue complication probabilities
are met. The choice of Δs_k will depend on personal preferences and the experience of dosimetrist and therapist. As a general principle, Δs_k should not be chosen too small in order to allow a flexible planning process. Due to the convexity of the EUD_k- and $\min_T$-functions, $\mathrm{PD}(S)$ is a convex set.

3 Pareto-optimal representatives in the planning domain

The most promising ξ in the planning domain $\mathrm{PD}(S)$ are those that are Pareto-optimal for (6), because these therapy plans cannot be improved for all costlets F_k at the same time. Therefore, let

$$\mathrm{Par}(S) := \{\xi \in \mathrm{PD}(S) \mid \xi \text{ is pareto for (6)}\}. \tag{9}$$

$\mathrm{Par}(S)$ is a coherent and bounded subset of the set of feasible solutions of problem (6). It will be the goal of this section to define a reasonable set of representative plans out of $\mathrm{Par}(S)$ that will satisfy a decision makers' need for choice. The representative system for $\mathrm{Par}(S)$ will be calculated in such a way that two basic principles are met:

- *Resolution:*
  The F-vectors of representatives are significantly different.

- *Homogeneity:*
  The representatives form a nearly equidistant cover of $\mathcal{F}(S) := F(\mathrm{Par}(S))$.

Even if possible, a complete description or calculation of $\mathrm{Par}(S)$ is far too costly on the one hand side and widely not interesting for the planner on the other hand, as therapy plans with too tiny F-differences are of identical worth for decision makers.
For the calculation of the representative set of $\mathrm{Par}(S)$ we propose a two phase algorithm. The first phase will find compromises in $\mathrm{PD}(S)$ that equibalance specific sets of so-called *active costlets* only. These plans are called *extreme*

compromises, because the active costlets will attain minimal values within $\mathrm{PD}(S)$ whereas the non-active costlets may exhaust the prescribed bounds of the planning domain. A second phase will care about reasonable resolution and homogeneity of the representative system and will appropriately place representatives in between the extreme compromises by means of an adaptive triangulation scheme.

3.1 Phase I - the extreme compromises

For any partition (M, N), $M \neq \emptyset$ of $\{T, R_1, \ldots, R_K\}$ we generate solutions of the problem

$$\begin{aligned} s &\rightarrow \text{Min} \quad \text{subject to} \\ F_k(\xi) &\leq s \quad \forall\, k \in M \\ F_k(\xi) &\leq s_k \quad \forall\, k \in N \\ \xi &\in \mathrm{Par}(S). \end{aligned} \tag{10}$$

With this setting, we will find therapy plans that give an equibalanced solution for active costlets F_k with indices $k \in M$, while the remaining non-active costlets with indices $k \in N$ satisfy the relaxed condition of merely staying in $\mathrm{Par}(S)$. Tentatively, the active costlet values will attain small values compared to non-active costlets. Therefore, we call a solution of (10) *extreme compromise* with respect to the active costlets with indices in M. However, a solution of (10) will not be uniquely determined in general. In order to avoid such ambiguities, we solve first the relaxed problem

$$\begin{aligned} s &\rightarrow \text{Min} \quad \text{subject to} \\ F_k(\xi) &\leq s \quad \forall\, k \in M \\ F_k(\xi) &\leq s_k \quad \forall\, k \in N \\ \xi &\geq 0 \end{aligned} \tag{11}$$

ending up with an optimal objective value s^*_M. Afterwards, we force Pareto-optimality and uniqueness of the solution by solving

$$\begin{aligned} \sum_{k \in \{T, R_1, \ldots, R_K\}} F_k &\rightarrow \text{Min} \quad \text{subject to} \\ F_k(\xi) &\leq s_k \quad \forall\, k \in N \\ F_k(\xi) &\leq s^*_M \quad \forall\, k \in M \\ \xi &\geq 0. \end{aligned} \tag{12}$$

The solution ξ_M of (12) will be called M-*extreme compromise* and

$$\mathcal{E}(S) := \{\xi_M \mid (M, N) \text{ partition of } \{T, R_1, \ldots, R_K\}, M \neq \emptyset\} \tag{13}$$

will denote the set of extreme compromises in $\mathrm{Par}(S)$.
Though extreme solutions might be seen as corner stone solutions among the relevant part of the objective space $\mathcal{F}(S) = F(\mathrm{Par}(S))$, $F(\mathrm{cone}(\mathcal{E}(S)))$ does in general not cover all but major parts of $\mathcal{F}(S)$ that are large enough to satisfy a decision makers' need for choice. As an advantage of this setting, the number of optimization problems that have to be solved for calculating $\mathcal{E}(S)$ is fixed and known beforehand as $2^{K+1} - 1$. This number only depends on the number of costlet functions and not on the complex geometry of $\mathcal{F}(S)$ or specific discretizations of the decision space.
We will restrict ourselves to generate a system of representatives that covers

$$\mathcal{F}_{\mathcal{E}}(S) := F(\mathrm{cone}(\mathcal{E}(S))) \cap \mathcal{F}(S) \tag{14}$$

in the following.

3.2 Phase II - generation of a ρ-cover

Starting with the extreme compromises that serve as corner stone solutions in the relevant area of the planning domain, we want to calculate a homogeneous set of representatives of $\mathcal{F}(S)$, that covers $\mathcal{F}_{\mathcal{E}}(S)$ at reasonable resolution. This is done with an adaptive triangulation scheme that introduces successively new representatives at places, where the current resolution or homogeneity is not sufficient. This is done by a two stage procedure. First, a basic triangulation scheme approximates $\mathcal{F}_{\mathcal{E}}(S)$ by simplices that are spanned as convex hulls of $K + 2$ neighboring extreme solutions. In a second step, this mesh of points is adaptively refined by introduction of new points from $\mathcal{F}_{\mathcal{E}}(S)$ that split too large simplices, cf. Figure (2). This procedure successively delivers a finer approximation of $\mathcal{F}_{\mathcal{E}}(S)$ and will be stopped when a ρ-cover of $\mathcal{F}_{\mathcal{E}}(S)$ has been constructed. A ρ-cover is a set of representative points in $\mathcal{F}_{\mathcal{E}}(S)$ such that any point of $\mathcal{F}_{\mathcal{E}}(S)$ lies within ρ-distance from at least one representative.

Basic triangulation: Each M-extreme compromise $\xi_M \in \mathcal{E}(S)$ can be identified with an incidence vector e_M, that has zero entries corresponding to active and one entries corresponding to non-active costlets. In this setting, $\mathcal{E}(S)$ maps one-to-one to the vertex set of a $(K+1)$-dimensional cube where the all-one-vertex is missing. It is easy to verify, that the partial order relation "$\leq$" of the F-vectors belonging to extreme compromises is isomorphic to that of the incidence vectors. Therefore, we can transfer a triangulation of the hypercube's surface to a triangulation of $\mathcal{F}_{\mathcal{E}}(S)$.

$\mathcal{F}_{\mathcal{E}}(S)$ corresponds to those facets of the unit hypercube that do not contain the all-one-vertex. Hence in order to triangulate $\mathcal{F}_{\mathcal{E}}(S)$ we dissect the associated $K + 1$ facets of the hypercube into simplices and reinterpret this triangulation in the objective space. Algorithmically, any of these simplices

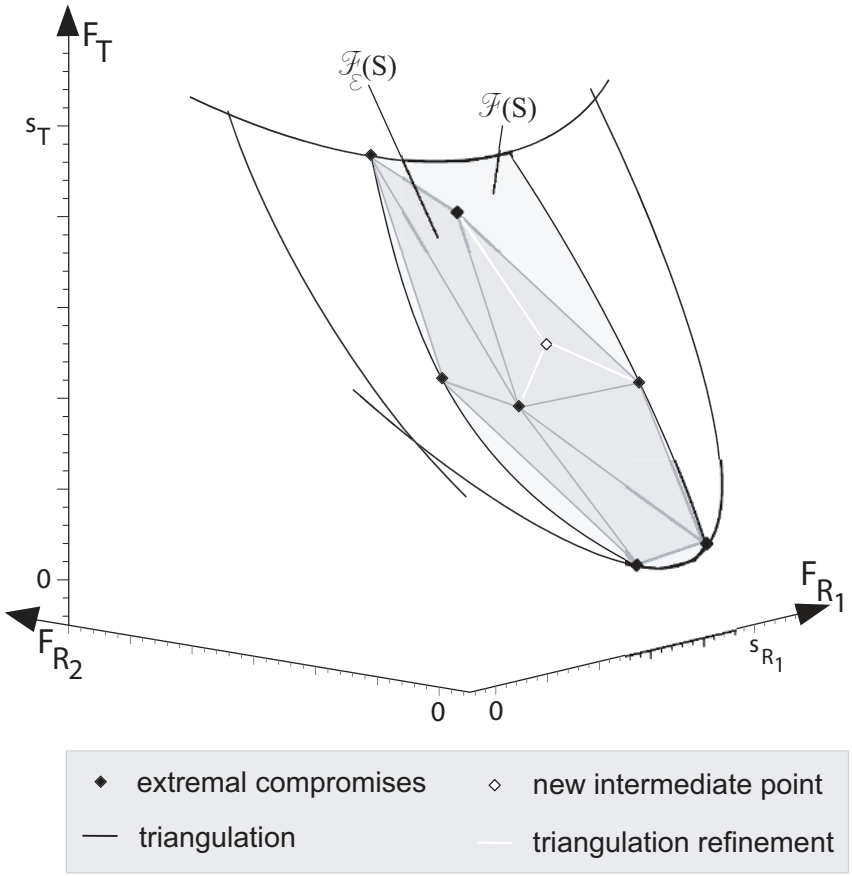

Figure 2: Covering the planning domain

can be identified with the convex hull of the column vectors of some permutation of the $(K+1) \times (K+1)$ matrix

$$\begin{pmatrix} 0 & 1 & \cdots & 1 \\ \vdots & \ddots & \ddots & \vdots \\ \vdots & & \ddots & 1 \\ 0 & \cdots & \cdots & 0 \end{pmatrix}.$$

Here, those simplices generated by matrices, whose k-th row consist of zero entries only, partition the k-th facet. If in a degenerate situation two or more extreme compromises coincide, we only reconsider proper simplices for further refinement and avoid duplicates.

Refinement step: The extreme solutions will be used as corner stone solutions of $\mathcal{F}_{\mathcal{E}}(S)$. It will be the objective of a refinement procedure to calculate an adaptive homogeneous ρ-cover that approximates $\mathcal{F}_{\mathcal{E}}(S)$. More precisely, we are looking for a mesh of points $\mathcal{R}_{\mathcal{E}}(\rho, S) \subset \mathcal{F}_{\mathcal{E}}(S)$ such that any point of $\mathcal{F}_{\mathcal{E}}(S)$ lies within ρ-distance from $\mathcal{R}_{\mathcal{E}}(\rho, S)$. The points of $\mathcal{R}_{\mathcal{E}}(\rho, S)$ are *representative solutions* of $\mathcal{F}_{\mathcal{E}}(S)$.
In order to achieve a ρ-cover we use a local criterion that ensures the covering properties. The simplest choice is to bisect edges of the current triangulation that are longer than ρ. The procedure stops, when there is no edge longer than ρ. This is a valid but clearly suboptimal choice with respect to computational complexity. More sophisticated rules lead to better computation times. We refer the interest reader to the literature on homogeneous mesh generation. Recent results and further reference on this topic can be found in [11]. Unfortunately, the convex combination of Pareto-optimal solutions, e.g. the midpoint of a long edge will in general not be Pareto-optimal. In this case we have to find a near-by Pareto-optimal point. In order to achieve this we use the following method:

Let $\bar{F}_k, k \in \{T, R_1, \ldots, R_K\}$ be entries of a costlet vector found as convex combination of Pareto-optimal solutions. We can find a neighboring Pareto-optimal representative solution by solving the optimization problem:

$$\begin{aligned} \theta &\rightarrow \text{Min} \quad \text{subject to} \\ F_T(\hat{\xi}) &\leq \theta(\bar{F}_T - 1) + 1 \\ F_k(\hat{\xi}) &\leq \theta(\bar{F}_k + 1) - 1 \quad k \in \{R_1, \ldots, R_K\} \\ \hat{\xi} &\in \text{Par}(S). \end{aligned} \tag{15}$$

The optimization setting (15) profits from the homogeneity of the EUDs. By changing of θ we move along a line in the objective space from the current convex combination $\bar{F}_k$ to the boundary of $\mathcal{F}(S)$.

3.3 The approximation algorithm for the planning domain

We summarize the algorithm described above:

PARETOPLAN

Input:

$L, u_1, \ldots, U_K, S, \rho$

Phase I:

Calculate all extreme compromises by enumerating the different partitions (M, N).

Phase II:

(a) Perform the basic triangulation.

(b) If no further refinement is needed, stop.

(c) Introduce a new solution where it is needed most (e.g. longest edge in the current cover).

(d) Split the affected simplices into appropriate sub-simplices.

(e) Goto (b).

Output:

ρ-cover $\mathcal{R}_{\mathcal{E}}(S, \rho)$

The given algorithm calculates the representative ρ-cover $\mathcal{R}_{\mathcal{E}}(S, \rho)$ of $\mathcal{F}_{\mathcal{E}}(S)$.

3.4 Some practical remarks

Complexity: Algorithms like PARETOPLAN that compute representations or approximations of the Pareto set of a multi-criteria optimization problem have in general a computational complexity that is exponential in the number of criteria. In our case, we have to solve exactly $2^{K+1} - 1$ convex optimization problems in Phase I. If we use a simple edge-bisection strategy for phase II the number of convex optimization problems to be solved will be

$$\mathcal{O}\left((K+1)\left(\frac{\text{longest edge}}{\frac{\rho}{2}}\right)^K\right). \tag{16}$$

This means for practical purposes that the number of criteria in use should not exceed 5 - 6.

Tradeoff-Entities: Unfortunately, in many clinical cases, e.g. tumors in the

brain, the number of entities under consideration will be larger. But it is observed in practice that typically no more than 4 - 5 organs at risk dominate the tradeoff discussion in a planning process. Hence, if we knew these *tradeoff-entities* afore, all other entities might be taken out of the objectives of problem (7) while we ensure that their EUDs remain below reasonable bounds. This will result in a considerably reduced computation time. But how can we find these tradeoff-entities? Here, a key-phenomenon is *correlation.*

Correlation: Two entities of interest are correlated, if worsening or improving one of them has a similar effect on the other. It is observed in practice that correlation effects are particularly relevant if many entities are involved. Correlation gives us a chance for reducing the set of tradeoff-entities. E.g. if two organs at risk are hit by the same combination of irradiation directions, they are highly correlated. If two entities are correlated, it is not necessary to include both into the set of tradeoff-entities. This can be used to reduce the number of organs included as optimization criteria and henceforth for a significant reduction of computation time. Algorithmically, we can exploit correlation phenomena in the following way: We start Phase I of the algorithm with all organs on stage as tradeoff-entities. During the run of Phase I correlation can be tested from time to time by use of appropriate correlation coefficients that measure dependences between different entities. If a significant threshold value for correlation is achieved the set of tradeoff-entities is appropriately reduced.

The choice of ρ: The parameter ρ is introduced in order to guarantee that the representative solutions' objective values form a homogeneous mesh in $\mathcal{F}_{\mathcal{E}}(S)$ which is on the one hand side coarse enough such that its meshpoints belong do distinguishable solutions (*Resolution*), but on the other hand dense enough to give a smooth representation (*Homogeneity*). A good choice of ρ will in practice be found adaptively during the run of the algorithm and is bounded from below by a preset value.

Discretization of optimization problems: The complexity of PARETOPLAN has been described alone in terms of the number of convex optimization problems to be solved in the course of the algorithm so far. But depending on the specification of these problems, the computational effort can be perceptibly different. First of all, the type of optimization problems to be solved can differ depending on the choice of the EUD functions. Using e.g. the Max&Mean-Model, all optimization problems to be solved can be represented as linear problems. In order to solve such problems with standard optimization algorithms we have to discretize these continuous problems. The way how these problems are discretized affects strongly the computation time. A detailed discussion of discretization strategies for the Max-&Mean Model can be found in Section 4. Similar considerations can be made for the p-Scale Model, which will be omitted.

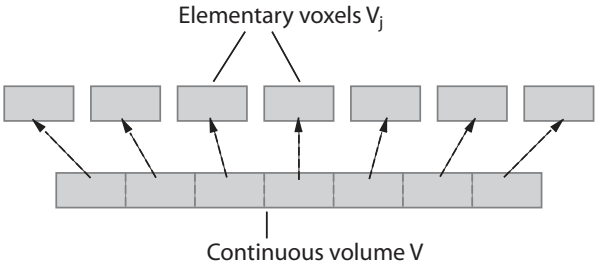

Figure 3: Schematic discretization of the volume

4 Discretization of the continuous problem

From now on, we will concentrate on the description of the Max & Mean-Model, where the mathematical structure profits a lot from linearity of the constraints.
In order to solve problems (7), (11), (12) and (15) numerically, one has to discretize body volume and beam head area appropriately. The necessary discretization will be twofold: First, we have to discretize the body - a 3D figure, and second, we have to discretize the beam heads - a 2D-figure.

4.1 Discretization of body volume and beam head area

Let $B = \bigcup_i B_i$, $V = \bigcup_j V_j$ denote partitions that divide the total beam head area B and the body volume V into small elements called *bixels* and *voxels*. These dissections are done in the following way:

The width of the leaf channels, cf. Figure 4, imply natural slices of B in one beam head dimension. Typically, these slices are dissected into quadratic bixels whose edge length is identical to the width of the leaf channel.
The size of the voxels is usually related to the distance between adjacent CT-slices. The relevant volume is cut into cubic voxels whose edge length corresponds to the distance of CT-slices, cf. Figure (3). Hence, we are dealing with a large scale optimization problem.

The continuous functions used for the description of the optimization problems in Section 3 are then discretized in the following way:
The fluence distribution $\xi(b)$ is replaced by a step function defined on the partition of B,

$$\xi(b) = \sum_i x_i 1_{B_i}(b), \tag{17}$$

and can thus be identified with a fluence vector $x = (x_i)$, where the i-th entry denotes the fluence value for bixel B_i, cf. Figure (4). With this notation the integral equation (1) turns into

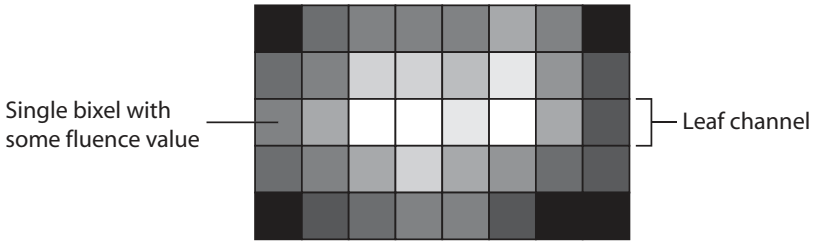

Figure 4: Schematic form of a fluence profile

$$d(\xi)(v) = \sum_i \int_{B_i} p(v,b)dbx_i =: \sum_i p(v,B_i)x_i =: d(x)(v), \tag{18}$$

where the continuous kernel function $p(v,b)$ is replaced by a vector-valued function $(p(v,B_i))_i$.

The partition of V in cubic voxels V_j allows to approximate $d(x)(v)$ by

$$D(x)(V_j) = \sum_i p(V_j,B_i)x_i, \tag{19}$$

where $p(V_j,B_i)$ denotes the dose deposit into voxel V_j from bixel B_i under unit fluence. We replace the kernel $p(v,b)$ by the matrix

$$P = (p_{ij}) = p(V_j,B_i), \tag{20}$$

and the dose distribution $d(\xi)(v)$ by a dose vector $D(x) = (D_j(x))$, whose j-th entry denotes the dose value in voxel V_j. The matrix-vector equation

$$D = D(x) = P \cdot x \tag{21}$$

becomes the discrete analogue of the integral equation (1). Altogether, both discretization steps lead to an approximate description of the continuous problems, where the discretization error is governed by the numerical approximation error of the kernel function.

4.2 The discrete problem

At first, we introduce discrete analogues of EUD_k and $\min_T$ in case of the Max & Mean Model:
Mean and maximum dose in the volume V_{R_k} of entity R_k are replaced by the corresponding discrete norms

$$\begin{aligned} \|D(x)\|_{\infty,k} &:= \max_{V_j \in V_{R_k}} \langle Px, e_j \rangle &&= \max_{V_j \in V_{R_k}} \langle x, P^t e_j \rangle \\ \|D(x)\|_{1,k} &:= |V_{R_k}|^{-1} \cdot \langle Px, e_{R_k} \rangle &&= \langle x, |V_{R_k}|^{-1} \cdot P^t \ 1_{R_k} \rangle, \end{aligned} \tag{22}$$

where e_j is the j-th unit vector and $1_{R_k} \in \{0,1\}^{|V_{R_k}|}$ with $(1_{R_k})_j = 1$ iff $V_j \in V_{R_k}$. With this notation the discrete EUD of V_{R_k} and the minimal dose in the target attain the forms

$$\begin{aligned} \mathrm{EUD}_k(D(x)) &= \alpha_k \cdot \|D(x)\|_{\infty,k} + (1-\alpha_k) \cdot \|D(x)\|_{1,k} \\ \min_T D(x) &= \min_{V_j \in V_T} \langle x, P^t e_j \rangle. \end{aligned} \tag{23}$$

These discrete reformulations of the problem preserve convexity and homogeneity of the continuous ancestor.
The continuous constraints from (4) change into the discrete voxel-related constraints

$$\begin{aligned} \langle x, c_j \rangle := \quad & \langle x, \alpha_k P^t e_j + (1-\alpha_k) N_k^{-1} P^t e_{R_k} \rangle \quad \leq U_k, \quad V_j \in V_{R_k} \\ \langle x, c_j \rangle := \quad & \langle x, P^t e_j \rangle \quad \geq L, \quad V_j \in V_T. \end{aligned} \tag{24}$$

Similar as in the continuous problem (7), a discrete least common tolerance value s^+ is obtained from

$$\begin{aligned} s &\rightarrow \text{Min} \quad \text{subject to} \\ F_k(x) &\leq s, \qquad k \in \{T, R_1, \ldots, R_K\} \\ x &\geq 0. \end{aligned} \tag{25}$$

Here, the optimal value s^+ depends on the choice of the discretization. The relative deviation F_k in problem (25)is defined by replacing EUD_k and $\min_T$ in (5) by their discretized counterparts (23). Finally, the discrete planning domain is defined by

$$\begin{aligned} \mathrm{PD}(S) := \{x \geq 0 : \quad & F_k(x) && \leq s_k, \ k = T, R_1, \ldots R_k\} \\ = \{x \geq 0 : \quad & \mathrm{EUD}_k(D(x)) && \leq U_k(1+s_k), \ k = R_1, \ldots R_k, \\ & \min_T D(x) && \geq L(1-s_T)\}, \end{aligned} \tag{26}$$

where $S := (s_k)$ with $s_k := s^+ + \Delta s_k$, $k \in \{T, R_1, \ldots, R_K\}$, $\Delta s_k > 0$. Due to the convexity of the constraints, $\mathrm{PD}(S)$ is a convex set. Discrete settings of problems (11), (12) and (15) are defined in a similar way.

4.3 Large-scale strategies using redundancy tests and clustering techniques

Obviously, the large number of constraints of type (24) makes the resulting linear programs large scale and the computational complexity intractable. Fortunately, the physical background of the problem provides some scope for decisive reduction. In a first stage we are going to detect redundant, unnecessary constraints, which will be kicked out from the problem description. In a second stage we fuse similar constraints successively to clusters in

such a way that the resulting reduced optimization problems serve as good approximation of the original one. Finally we find the optimal solution of the original problem with a local refinement procedure.

Redundancy of constraints: We observe that neighboring voxels V_{j_1}, V_{j_2} in an organ are irradiated by the same bixels with quite similar dose deposits in general. Hence, the corresponding normal vectors c_{j_1}, c_{j_2} of the constraints in (24) do not differ too much. Since the right hand sides of these constraints, i.e. the upper and lower bounds for the dose values, are constant for each entity, the similarities of the left hand sides cause a quite large percentage of redundancy. The simplest form of redundancy is a one-to-one domination of constraints, i.e. a constraint is dominated by a single other constraint. This occurs especially in the penumbra of the target:
Let e.g. $V_{j_1}, V_{j_2} \in V_{R_k}$ and $U \geq 0$ be some upper bound in V_{R_k}, then for any feasible $x \geq 0$ we have

$$\langle x, c_{j_1} \rangle, \langle x, c_{j_2} \rangle \leq U. \tag{27}$$

If now $c_{j_1} \leq c_{j_2}$ holds componentwise this implies

$$\langle x, c_{j_1} \rangle \leq \langle x, c_{j_2} \rangle \leq U. \tag{28}$$

Thus, the constraint corresponding to voxel V_{j_1} is dominated by the constraint associated to voxel V_{j_2}. Such simple forms of redundancy can be efficiently detected and eliminated, what results in a significant reduction of the problem size. From now on, we restrict ourselves to the remaining (not found redundant) voxels, but for the sake of simplicity denote them as "all voxels" and transfer the original notations like e.g. V and V_{R_k} to them.
A recent survey on redundancy detection in linear programming can be found e.g. in [1].

Similarity of constraints and clustering: Beyond elimination of redundancies there is still substantial potential for reduction of the problem size. An immediate idea to exploit similarity of constraints is to fuse only slightly different constraints belonging to neighboring voxels of an organ in representative constraints. More precisely, let V_ι, $\iota \in \mathcal{J}$, denote the set of remaining voxels of an entity V with their corresponding constraint vectors c_ι. Assume that

$$\{V_\iota : \ \iota \in \mathcal{J}_j\}, \quad \mathcal{J}_j \subset \mathcal{J} \tag{29}$$

is a family of voxels with almost identical associated constraints. We fuse the voxels of this family to a *voxel cluster*

$$V_j' := \bigcup_{\iota \in \mathcal{J}_j} V_\iota \tag{30}$$

and form a normal vector c'_j representing the constraint vectors $\{c_\iota : \iota \in \mathcal{J}_j\}$, which implies a feasible constraint. This means, that the inequalities $\langle x, c_\iota \rangle \leq U$ are replaced by the valid inequality $\langle x, c'_j \rangle \leq U$. We get a *cluster* (V'_j, c'_j). If we apply this method to the relevant volume we obtain a *clustering*

$$\mathcal{C} := \{(V'_j, c'_j) : \ j \in \mathcal{J}'\}, \quad \bigcup_{j \in \mathcal{J}'} \mathcal{J}_j = \mathcal{J}. \tag{31}$$

We now apply this clustering procedure in order to replace the original problem description with voxel oriented constraints of type (24) by cluster oriented constraints. Clustering will perturbe the original planning domain PD(S) from (26) and the evaluation functions F_k slightly. Hence, a clustering procedure will replace the original optimization problems by approximations.
Using clusterings, the computational expense necessary to find optimal dose distributions can be significantly reduced: a fine resolution (the finest available is given by the natural voxel and bixel sizes defined above) is only used in some critical volume parts, in which the requirements are rather difficult to fulfill, e.g. the seam of the target. A much coarser resolution can be used in all minor critical volume parts, e.g. in volumes farther away from the focus of the radiation beams.
As it is hard to decide beforehand, which parts of the relevant volume will be critical, a clustering strategy must provide the possibility for a future local approximation. This requires the availability of a *hierarchy of clusterings* with different resolution. In order to construct such a hierarchy we use the subsequent algorithmic scheme:

Starting off with the trivial clustering $\mathcal{C}^{(0)}$ based on the original non-redundant voxels and constraints, i.e. $V_j^{(0)} = V_j$, $c_j^{(0)} = c_j$ and $\mathcal{J}^{(0)} = \mathcal{J}$, we construct step-by-step a hierarchy of clusterings

$$\mathcal{C}^{(l)} := \{(V_j^{(l)}, c_j^{(l)}) : \ j \in \mathcal{J}^{(l)}\}, \quad l = 0, 1, \ldots, l_{max} \tag{32}$$

by fusion of clusters $V_j^{(l-1)}$ and aggregation of constraints $c_j^{(l)}$ based on reasonable partitions of the index sets under consideration

$$\bigcup_{j \in \mathcal{J}^{(l)}} \mathcal{J}_j^{(l-1)} = \mathcal{J}^{(l-1)}, \tag{33}$$

cf. Figures (5,6).

In order to define a hierarchy of clusterings we use a *clustering strategy* that is guided by the following principles: different entities have different clustering hierarchies adapted to the sensitivity of radiation of the organ under consideration. Clusters close to the focus of the radiation beams will

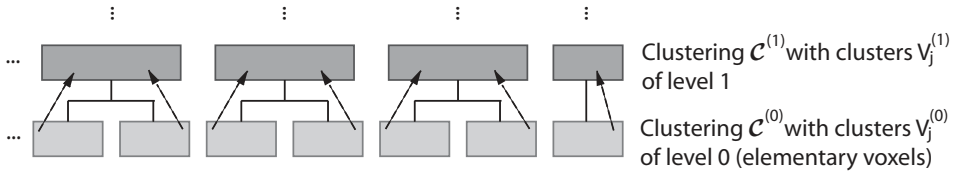

Figure 5: Scheme of the clustering process

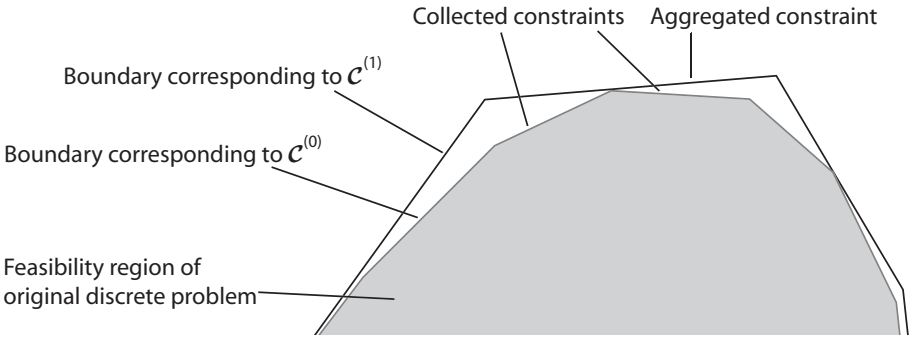

Figure 6: Approximation of the planning domain

in general be finer than those farther away. Altogether we obtain a collection of clusterings

$$\left\{\mathcal{C}_k^{(l)} :\ l = 0, \ldots, l_{max}(k),\ k = T, R_1, \ldots R_K\right\}. \tag{34}$$

Mathematically, a clustering strategy is determined by appropriately chosen organ dependent sequences of *tolerance levels*

$$0 < \delta_k^{(1)} < \delta_k^{(2)} < \ldots < \delta_k^{(l_{max})}. \tag{35}$$

We put together clusters $V_\iota^{(l-1)} \subset V_{R_k}$ and form a cluster $(V_j^{(l)}, c_j^{(l)})$ with $V_j^{(l)} = \bigcup V_\iota^{(l-1)}$, if

$$\max_{V_\iota \subset V_j^{(l)}} \Delta(c_\iota, c_j^{(l)}) \leq \delta_k^{(l)}. \tag{36}$$

Thus, we fuse voxels and constraint vectors to clusters in level l, if the distances between the constraint vectors of the voxels and the aggregated constraint vector in an appropriately chosen metric Δ do not exceed the tolerance level $\delta_k^{(l)}$. As mentioned above, clustering will affect the evaluation

functions F_k. We therefore introduce evaluation functions $F_k^{(l)}$ corresponding to level l. The errors between these *level evaluation functions* $F_k^{(l)}$ and the original function $F_k = F_k^{(0)}$ restricted to a voxel-cluster $V_j^{(l)}$ (what is denoted as $F|_{V_j^{(l)}}$) fulfill

$$\begin{aligned} \left| (F_k^{(l)} - F_k)|_{V_j^{(l)}}(x) \right| &= \left| \max_{V_\iota \subset V_j^{(l)}} \left[F_k^{(l)}|_{V_\iota}(x) - F_k|_{V_\iota}(x) \right] \right| \\ &= \max_{V_\iota \subset V_j^{(l)}} \left| \langle x, c_j^{(l)} \rangle - \langle x, c_\iota \rangle \right| \\ &\leq \|x\|_2 \cdot C_\Delta \cdot \delta_k^{(l)} =: \varepsilon_k^{(l)} \end{aligned} \tag{37}$$

with some metric dependent constant C_Δ. The clustering and the local refinement procedure in the optimization algorithm will be controlled with tolerance levels $\varepsilon_k^{(l)}$ in the objective space.

Local refinement using a cutting plane strategy: After having coarsened the problem in total by clustering, we now will find a solution of the original problem by a *local approximation scheme* that refines the problem description close to the optimal solution. The concept is heavily related to cutting plane approximates schemes known from discrete optimization where the discrete polyhedron is approximated with successively constructed real polyhedra starting with a continuous relaxation of the original problem.
For the sake of simplicity of notation, we will explain the basic ideas in case of the solution of least common tolerance (7), i.e.

$$\begin{aligned} & & s &\rightarrow \text{Min} \quad \text{subject to} \\ LP: \quad & F_k(x) &\leq s, \qquad & k \in \{T, R_1, \ldots, R_K\}, \\ & x &\geq 0. & \end{aligned} \tag{38}$$

that will be denoted in the sequel by LP. The corresponding set of optimal solutions - in general the solution of (38) will not be uniquely determined - is denoted by $\tilde{X}$. An extension to problems (11), (12) or (15) is straightforward.

We construct a series of approximations of (LP) based on sets $\mathcal{A}(t)$ defined by

$$\mathcal{A}(t) \subset \bigcup_{k=T,R_1,\ldots R_K} \; \bigcup_{l=0,\ldots,l_{max}(k)} \mathcal{C}_k^{(l)}, \quad t = 0, 1, \ldots, \tag{39}$$

that consist of previously constructed clusters. More precisely

$$\bigcup_{k=T,R_1,\ldots R_K} V_k = \bigcup_{(V_\alpha, c_\alpha) \in \mathcal{A}(t)} V_\alpha, \tag{40}$$

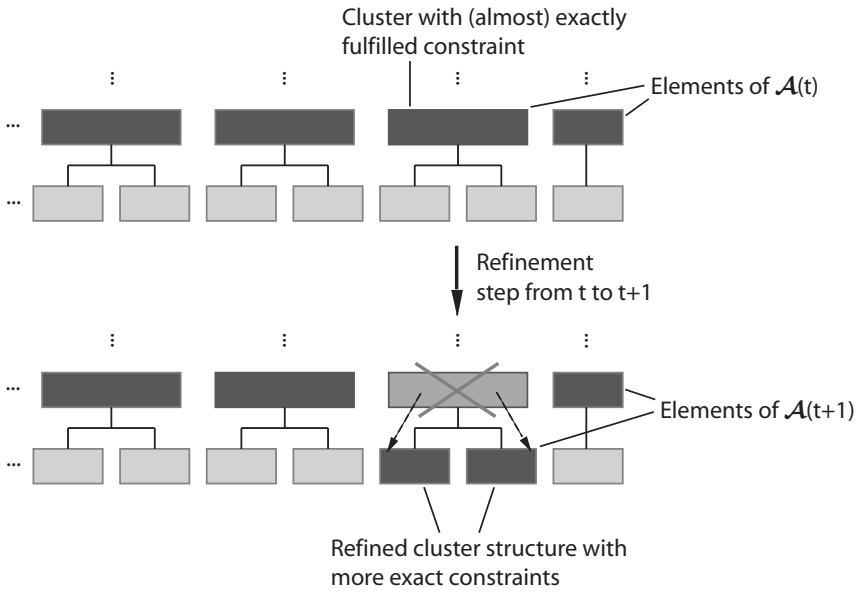

Figure 7: Local refinement of the clustering

i.e. the sets in $\mathcal{A}(t)$ form a partition of the relevant body volume like the clustering. With increasing t the resolution of $\mathcal{A}(t)$ will become higher. This means in particular, we call $\mathcal{A}(t_2)$ finer as $\mathcal{A}(t_1)$,

$$\mathcal{A}(t_2) \prec \mathcal{A}(t_1), \quad t_1 < t_2, \tag{41}$$

if for all $(V^{(t_2)}, c^{(t_2)}) \in \mathcal{A}(t_2)$ there exists a $(V^{(t_1)}, c^{(t_1)}) \in \mathcal{A}(t_1)$ such that $V^{(t_2)} \subseteq V^{(t_1)}$ and $|\mathcal{A}(t_2)| > |\mathcal{A}(t_1)|$, cf. Figure (7). The approximation scheme $\{\mathcal{A}(t)\}$ starts off with

$$\mathcal{A}(0) = \bigcup_{k=T,R_1,\ldots,R_K} \mathcal{C}_k^{(l_{max}(k))}, \tag{42}$$

which corresponds to the coarsest clustering of each organ of interest. In case of the other problems (11), (12) or (15), one takes the final approximation corresponding to the previously solved problem.

Each approximation $\mathcal{A}(t)$ yields an approximate formulation

$$\begin{array}{rrcll} & s & \to & \text{Min} & \text{subject to} \\ LP(t): & F_k^{(\mathcal{A}(t))}(x) & \leq & s, & k \in \{T, R_1, \ldots, R_K\}, \\ & x & \geq & 0. & \end{array} \tag{43}$$

of problem (38). The objective functions $F_k^{(\mathcal{A}(t))}$ are adapted to the approximation and are analogously defined as the level-based ones in (37). The

associated set of optimal solutions of $LP(t)$ is denoted by $\tilde{X}(t)$.
The refinement step going from $\mathcal{A}(t)$ to $\mathcal{A}(t+1)$ is done in the following way:
If we detect an active or almost active constraint associated to some cluster(s) of $\mathcal{A}(t)$ for an optimal solution $\tilde{x}(t) \in \tilde{X}(t)$ of $LP(t)$, these active or almost active clusters will be replaced by a finer partition in the cluster hierarchy. Geometrically, when going from t to $t+1$ and so on, we successively cut off parts from the feasibility region of $LP(t)$ in a neighbourhood of $\tilde{X}$, cf. Figure 8. Henceforth, by going down in the cluster hierarchy we locally approximate the set of feasible solutions of LP close to $\tilde{X}$. In terms of the objective functions this means

$$F_k(\tilde{X}(t)) \to F_k(\tilde{X}) \quad \text{for} \quad t \to \infty, \quad k = T, R_1, \ldots, R_K. \tag{44}$$

Moreover, all constraints defining the boundary of the domain of LP close to $\tilde{X}$, are gradually detected and added to $LP(t)$.
Due to the finite description of the clustering hierarchy the refinement process will stop after a finite number of steps with $\mathcal{A}(t_{stop})$. This final approximation gives an approximation $LP(t_{stop})$ of LP with $\tilde{X}(t_{stop}) = \tilde{X}$.
The described process of local approximation close to $\tilde{X}$ of LP provides will solve the original problem X exactly, but with a significantly reduced expected computational expense.

To describe precisely the refinement step, let us assume that $\tilde{x}(t)$ almost exactly fulfills the associated constraint to some voxel-cluster $V_j^{(l+1)} \subset V_{R_k}$ in $\mathcal{A}(t)$, i.e.

$$s_k - \varepsilon_k^{(l+1)} < F_k^{(l+1)}|_{V_j^{(l+1)}}(\tilde{x}(t)) \leq s_k \tag{45}$$

with some upper bound $s_k \geq 0$. This might - according to (37) - result in $s_k < F_k|_{V_{\iota''}}(\tilde{x}(t))$ in some voxel $V_{\iota''} \subseteq V_{\iota'}^{(l)} \subset V_j^{(l+1)}$.
We replace $c_j^{(l+1)}$ by tighter constraints $c_\iota^{(l)}$ corresponding to subclusters and hereby introduce hyperplanes that cut off some volume part of the feasible domain of $LP(t)$. As the feasible domain of LP is always a subset of the domain of $LP(t)$ we improve the approximation of the domain of LP, cf. Figure (8).
If

$$s_k - \varepsilon_k^{(l+1)} < F_k^{(l)}|_{V_j^{(l+1)}}(\tilde{x}(t)) \leq s_k - \varepsilon_k^{(l)} < s_k, \tag{46}$$

holds, no further refinement will be needed, since then

$$F_k|_{V_\iota}(\tilde{x}(t)) < s_k \tag{47}$$

for all $V_\iota \subseteq V_j^{(l+1)}$.

For related literature on the general concept of cluster analysis the interested reader is referred to [6]. For the more specific case of large-scale handling in

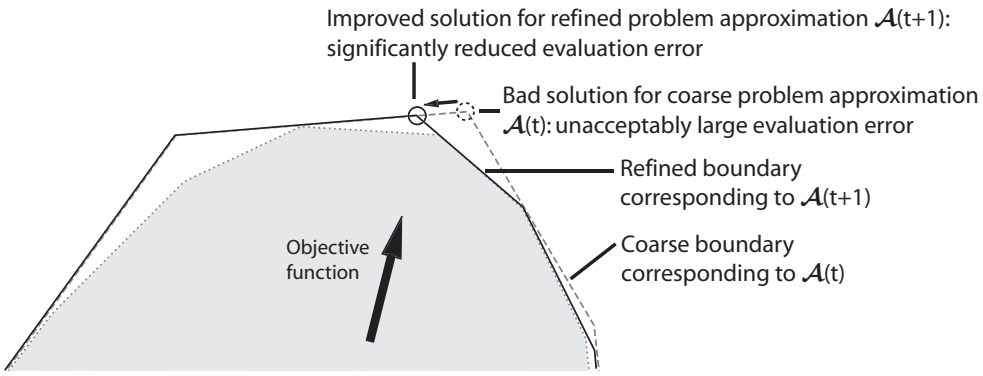

Figure 8: Improving the approximation quality

optimization problems using aggregation and disaggregation techniques an extensive survey can be found in [4].

4.3.1 The local approximation algorithm

The following formal description gives a survey on the aggregation and disaggregation processes designed for solving the optimization problems from Section 3.

LOCALAPPROX

Input:

LP of form (38)

Phase I:

Loop over all organs.

Detect and eliminate redundant constraints in the current organ.

Phase II:

Loop over all organs.

a) $l \leftarrow 0$.

b) If $l > l_{max}$ stop.

c) Cluster the elements on level l.

d) $l \leftarrow l + 1$.

e) Goto (b).

Intermediate Output:

Hierarchy of clusterings for the relevant volume parts in each organ.

Phase III (integrated in the computation of one solution):

a) $t \leftarrow 0$. Initialize $\mathcal{A}(t)$.

b) Compute an optimal solution $\tilde{x}(t)$ for $\mathcal{A}(t)$.

c) If there are no (almost) active clusters, $\tilde{x} \leftarrow \tilde{x}(t)$ and stop.

d) Split up (almost) active clusters. $t \leftarrow t + 1$.

e) Goto (b).

5 The data base of representative solutions in the planning domain

A major advantage of the multi-criteria approach to radiation therapy planning is the variety of solutions provided to the decision maker. Algorithm PARETOPLAN, cf. Section 3, will calculate in batch mode a number, typically around 1000, of Pareto-optimal solutions in the planning domain that will serve as data stack for the decision process. Of course a clinical decision maker cannot check all information provided without the support of an appropriate navigation tool, that enables a fair and fast comparison between different radiation therapy plans. In order to define such a navigation tool data must be structured.

5.1 Structure of the data base

Each patient to be treated will be associated a data base of personal treatment information that contains the following information sections:

- *General:*
  Name, age, anamnesis etc.
- *Geometric:*
  CT-, MRI-, Ultrasound-Images etc. with organ segmentation.
- *Dose:*
  Dose distribution matrix for the relevant body volume, dose-volume-histograms, EUD-levels.
- *Setup:*
  Irradiation geometry, intensity maps, MLC sequencing.

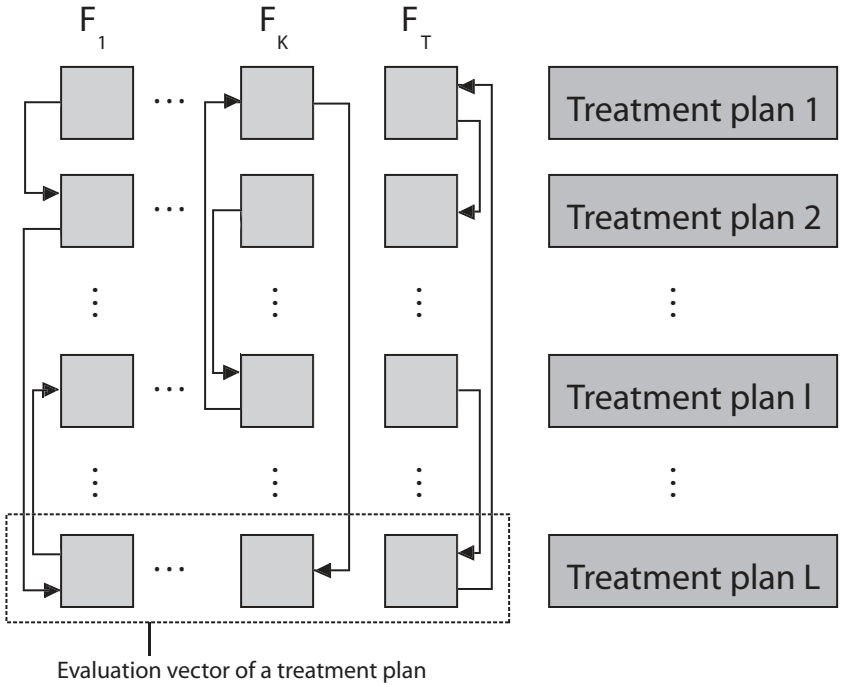

Figure 9: Structure of the database

The first sections, general and geometric information, are static and independent from the choice of a particular treatment plan, whereas the last sections, dose and setup information, are dynamic and dependent from the treatment plan. The treatment plans in the data base will be assessed and compared with regard to their dose information. The generation of the data base in algorithm PARETOPLAN was controlled by choices of meaningful EUD-levels. Therefore it is natural that the information in the data base is ordered by use of these EUD-levels. In Section 2, we associated each plan a vector of EUD-levels or F-vectors that characterizes the dose distribution. The plans in the data base are ordered with respect to ascending EUD-levels F_k for all $k \in \{T, R_1, \ldots, R_K\}$, cf. Figure 9. So, for each specific solution, the k-neighbors, i.e. solutions with neighboring F_k levels, are known. This knowledge will be exploited for the design of a navigation tool.

5.2 Data visualization and navigation

The planning screen provided to the decision maker, cf. Figure 10, reflects the structure of the data base. It consists of three major frames, the first frame on the upper right shows general patient information, the second frame on the lower right shows the EUD-navigator, while the third frame visualizes the dose distribution. The solution under consideration is shown by a hierarchy of dose information: coarsest information is given by the

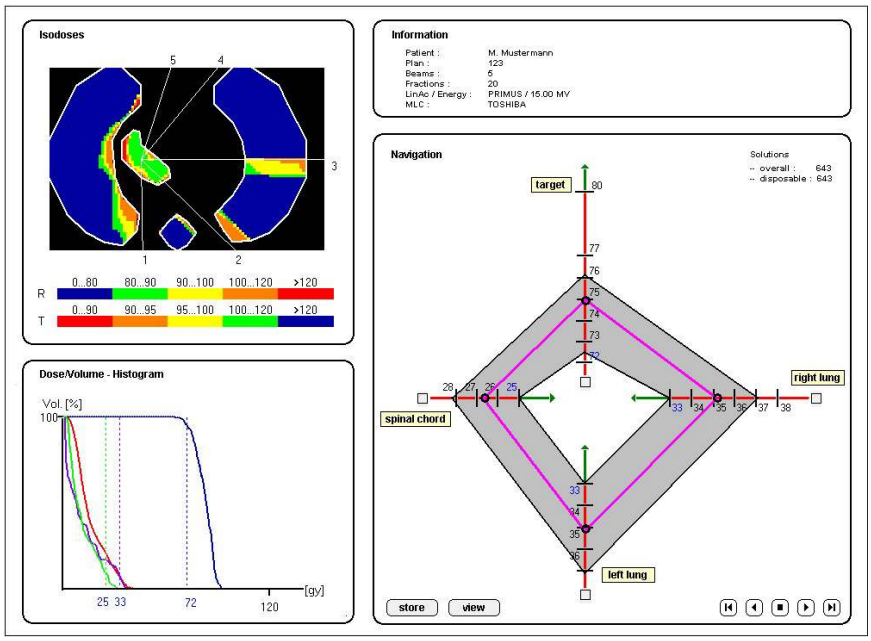

Figure 10: The planning screen

EUD-levels in the navigation frame, cf. Figure 11, that provides some organ structure dependent average dose values (EUDs) for each entity of interest. The particular EUD-levels for the current solution represented as vertices of the navigation polygon in the navigation frame. All vertices lie on a star coordinate system, cf. [10], that represents the objective space. The shaded area in the navigation window visualizes the variety of solutions stored in the data base and gives the EUD-levels that are covered by the planning domain explored by PARETOPLAN. Finer information is given by the dose volume histogram that relates dose levels to those volume shares where these doses will be achieved. Finest information is provided by 2D(3D)-visualizations of the dose distributions by use of color wash dose distributions or a bunch of isodose curves.

Planning details will be explained by a typical navigation session:
The medical decision maker starts the program, identifies the patient and obtains a planning screen, cf. Figure 10, that shows as starting proposal a solution of least common tolerance (7).
Now, navigation in the data base will consist of two phases: in a first phase the clinician will find acceptable EUD-levels within the planning domain visualized by the navigation frame. This will end in a *preset solution*, that is found by use of EUD-levels alone. In a second phase the clinician will find the final radiation therapy plan with the aid of a fine-tuning process supported by dose volume histograms and visualizations of isodose curves.

The preset solution: EUD-levels of the current solution are detected as vertices of the navigation polygon in the navigation frame. These vertices serve as handles for navigation in the planning domain. If the clinician is not satisfied with the EUD-configuration of the current solution he will move the handle belonging to a non-satisfying EUD towards a more promising area of the planning domain. During this process he will observe the move of the other vertices of the navigation polygon. At least one EUD-level will be worsened, as all solutions in the data base are Pareto. This means: there is no improvement for one EUD-level without worsening some other. The search process is facilitated by a *lock function*. Locking a specific EUD-level, for organ k say, means that the clinician does not want to see solution whose EUD-values with respect to organ k are worse than the currently observed level. When locking EUD-values all solutions in the data base with worse EUD-levels become inactive. In the navigation frame the area corresponding to plans with worse k-th EUD-levels is shaded. This means, by using locks the decision maker will focus his attention more and more to the interesting parts of the planning domain. Nevertheless, locks might be released in the future planning progress in order to reactive solutions of the already locked planning domain and thus enabling different compromises, if necessary. The complete process for finding a preset solution will consist of a sequence of moving, lock or unlock functions until a compromise of interest has been found. In practice, this preset procedure will typically take no more than five minutes. Additional storing and monitoring functions enable the administration of promising therapy plans.

The fine-tuning procedure: When having found an acceptable configuration of EUDs in a preset solution, the specific local dose distribution can be assessed by use of dose volume histograms and isodose curves. If the clinician is not satisfied with some histogram function or some isodose curve he might draw borderlines or dose volume wedges in the dose volume histogram or might highlight areas of discontent in some isodose visualization, cf. Figure 10. When clicking on these indicators, borderlines, wedges or highlighted areas, the system will search in the neighborhood of the currently proposed plan in order to improve the situation as well as possible without a significant change of the current EUD-configuration. Discussion of stored preset solutions and fine-tuning process will take between 15 and 30 minutes depending on the complexity of the specific case and the expertise of the planning clinician.

6 Numerical experience and concluding remarks

The authors are running projects funded by Deutsche Krebshilfe and the German Federal Ministry for Education and Science.

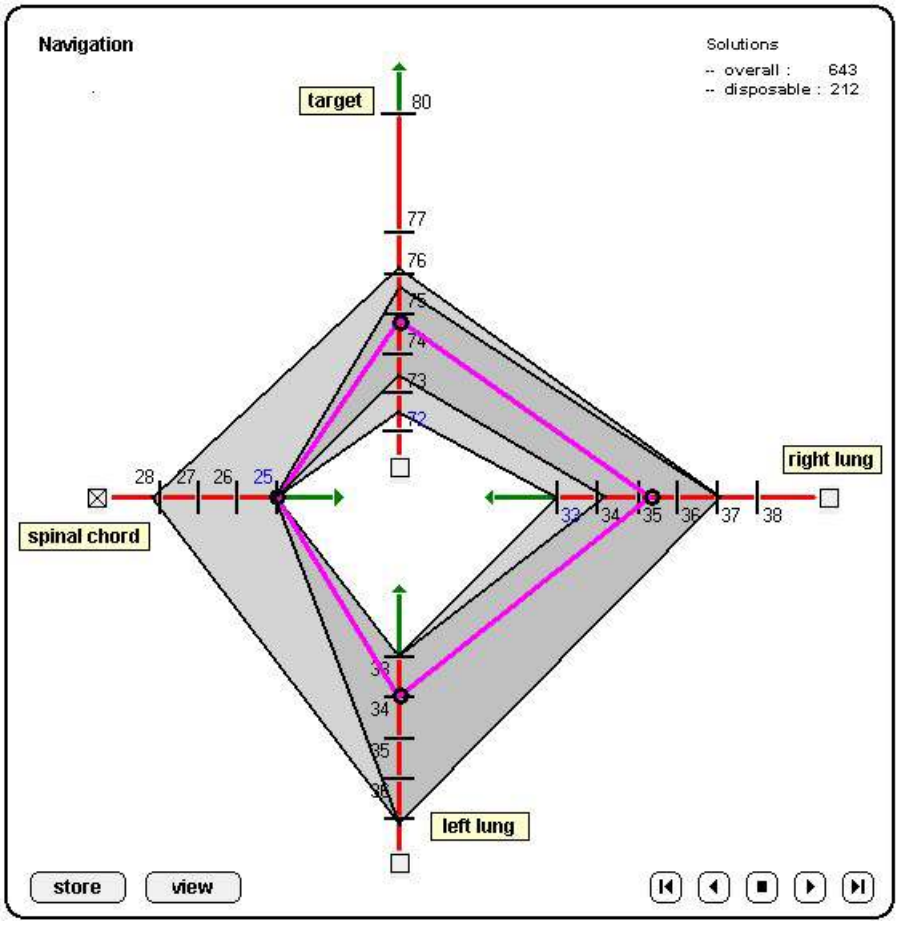

Figure 11: The navigation tool

A 3D-prototype software for the multi-criteria based planning of radiotherapy using the algorithms proposed in this paper has been implemented and was applied to real clinical data. According to the discretization from Section 4.1, the size of these problems ranged from 300000 to 450000 voxels and from 400 to 1900 bixels. Elimination of all voxels found redundant resulted in a remaining original problem with a size reduction between 10 and 40 percent and the organ specific clustering hierarchies consisted of 3 to 5 levels, cf. Section 4.3. The size of the approximate problem formulation based on the clusters of highest level was less than 10 percent of the size of the remaining original problem.
In the case of the calculation of the solution of least common tolerance, cf. Section 2.2, the approximation scheme from Section 4.3 required between 10 and 20 steps of local refinement and resulted in an approximate problem formulation with 10 to 15 percent of the size of the remaining original problem. For the computation of each of the extreme solutions, cf. Section 3.1, the approximation scheme required between 0 and 7 further refinement steps when starting off with the approximation of the precedingly calculated solution. Although already refined cluster structures are kept even when getting uncritical, the size of the finally resulting approximate problem formulation changed only moderately and did not exceed 20 percent of the size of the remaining problem. The computation of all other solutions, cf. Section 3.2, required only few further refinements, thus increasing the problem size only slightly.
The computation was done using the commercial solver ILOG CPLEX 7.5 under Linux on a 2.0 GHz Pentium IV platform with 2GB RAM. The computing time for the definition of the data base ranged between 2 and 5 hours CPU-time.

A commercial release of the software is planned and will be published with a German industrial partner tentatively in dawn 2003. For the functionality of the navigation tool described in Section 5, an international patent is pending. Further information, e.g. a movie showing an example of a planning session, can be found on the project page http://www.itwm.fhg.de/radioplan.

References

[1] Arnon Boneh, Shahar Boneh, and Richard J. Caron. Redundancy. In Tomas Gal et al., editor, *Advances in sensitivity analysis and parametric programming*, volume 6 of *International Series in Operations Research and Management Science*, chapter 13, pages 1–41. Kluwer Academic Publishers, 1997.

[2] T. Bortfeld, J. Stein, and K. Preiser. Clinically relevant intensity modulation optimization using physical criteria. In D.D. Leavitt and

G. Starkschall, editors, *Proceedings of the XIIth ICCR, Salt Lake City 1997*, pages 1–4, 1997.

[3] C. Burman, G.J. Kutcher, B. Emami, and M. Goitein. Fitting of normal tissue tolerance data to an analytic function. *Int. J. Radiat. Oncol. Biol. Phys.*, 21:123–135, 1991.

[4] James Evans, Robert D. Plante, David F. Rogers, and Richard T. Wong. Aggregation and disaggregation techniques and methodology in optimization. *Operations Research*, 39(4):553–582, 1991.

[5] H.W. Hamacher and K-H. Küfer. Inverse radiation therapy planning - a multiple objective optimization approach. *Discrete Applied Mathematics*, 118:145–161, 2002.

[6] Pierre Hansen and Pierre Jaumard. Cluster analysis and mathematical programming. *Mathematical Programming*, 79:191–215, 1997.

[7] K-H. Küfer, H.W. Hamacher, and T.R. Bortfeld. A multicriteria optimization approach for inverse radiotherapy planning. In T.R. Bortfeld and W. Schlegel, editors, *Proceedings of the XIIIth ICCR, Heidelberg 2000*, pages 26–29, 2000.

[8] G.J. Kutcher and C. Burman. Calculation of complication probability factors for non-uniform normal tissue irradiation: The effective volume method. *International Journal of Radiation Oncology, Biology and Physics*, 16:1623–1630, 1989.

[9] J.T. Lyman and B. Wolbarst. Optimization of radiation therapy iii: a method of assessing complication probabilities from dose-volume histograms. *International Journal of Radiation Oncology, Biology and Physics*, 13:103–109, 2002.

[10] K. Miettinen. *Nonlinear Multiobjective Optimization*. Kluwer, Boston, 1999.

[11] S.A. Mitchell and S.A. Vavasis. Quality mesh generation in higher dimensions. *SIAM Journal on Computing*, 29:1334–1370, 2000.

[12] A. Niemierko. A generalized concept of equivalent uniform dose. *Med. Phys.*, 26:1100, 1999.

[13] R. Steuer. *Multicriteria Optimization: Theory, Computation and Applications*. Wiley, NewYork, 1985.

[14] C. Thieke, T.R. Bortfeld, and K-H. Küfer. Characterization of dose distributions through the max and mean dose concept. *Acta Oncologica*, 41:158–161, 2002.

Published reports of the Fraunhofer ITWM

The PDF-files of the following reports are available under:
www.itwm.fraunhofer.de/zentral/berichte.html

1. D. Hietel, K. Steiner, J. Struckmeier

A Finite - Volume Particle Method for Compressible Flows

We derive a new class of particle methods for conservation laws, which are based on numerical flux functions to model the interactions between moving particles. The derivation is similar to that of classical Finite-Volume methods; except that the fixed grid structure in the Finite-Volume method is substituted by so-called mass packets of particles. We give some numerical results on a shock wave solution for Burgers equation as well as the well-known one-dimensional shock tube problem.
(19 pages, 1998)

2. M. Feldmann, S. Seibold

Damage Diagnosis of Rotors: Application of Hilbert Transform and Multi-Hypothesis Testing

In this paper, a combined approach to damage diagnosis of rotors is proposed. The intention is to employ signal-based as well as model-based procedures for an improved detection of size and location of the damage. In a first step, Hilbert transform signal processing techniques allow for a computation of the signal envelope and the instantaneous frequency, so that various types of non-linearities due to a damage may be identified and classified based on measured response data. In a second step, a multi-hypothesis bank of Kalman Filters is employed for the detection of the size and location of the damage based on the information of the type of damage provided by the results of the Hilbert transform.
Keywords: Hilbert transform, damage diagnosis, Kalman filtering, non-linear dynamics
(23 pages, 1998)

3. Y. Ben-Haim, S. Seibold

Robust Reliability of Diagnostic Multi-Hypothesis Algorithms: Application to Rotating Machinery

Damage diagnosis based on a bank of Kalman filters, each one conditioned on a specific hypothesized system condition, is a well recognized and powerful diagnostic tool. This multi-hypothesis approach can be applied to a wide range of damage conditions. In this paper, we will focus on the diagnosis of cracks in rotating machinery. The question we address is: how to optimize the multi-hypothesis algorithm with respect to the uncertainty of the spatial form and location of cracks and their resulting dynamic effects. First, we formulate a measure of the reliability of the diagnostic algorithm, and then we discuss modifications of the diagnostic algorithm for the maximization of the reliability. The reliability of a diagnostic algorithm is measured by the amount of uncertainty consistent with no-failure of the diagnosis. Uncertainty is quantitatively represented with convex models.
Keywords: Robust reliability, convex models, Kalman filtering, multi-hypothesis diagnosis, rotating machinery, crack diagnosis
(24 pages, 1998)

4. F.-Th. Lentes, N. Siedow

Three-dimensional Radiative Heat Transfer in Glass Cooling Processes

For the numerical simulation of 3D radiative heat transfer in glasses and glass melts, practically applicable mathematical methods are needed to handle such problems optimal using workstation class computers. Since the exact solution would require super-computer capabilities we concentrate on approximate solutions with a high degree of accuracy. The following approaches are studied: 3D diffusion approximations and 3D ray-tracing methods.
(23 pages, 1998)

5. A. Klar, R. Wegener

A hierarchy of models for multilane vehicular traffic
Part I: Modeling

In the present paper multilane models for vehicular traffic are considered. A microscopic multilane model based on reaction thresholds is developed. Based on this model an Enskog like kinetic model is developed. In particular, care is taken to incorporate the correlations between the vehicles. From the kinetic model a fluid dynamic model is derived. The macroscopic coefficients are deduced from the underlying kinetic model. Numerical simulations are presented for all three levels of description in [10]. Moreover, a comparison of the results is given there.
(23 pages, 1998)

Part II: Numerical and stochastic investigations

In this paper the work presented in [6] is continued. The present paper contains detailed numerical investigations of the models developed there. A numerical method to treat the kinetic equations obtained in [6] are presented and results of the simulations are shown. Moreover, the stochastic correlation model used in [6] is described and investigated in more detail.
(17 pages, 1998)

6. A. Klar, N. Siedow

Boundary Layers and Domain Decomposition for Radiative Heat Transfer and Diffusion Equations: Applications to Glass Manufacturing Processes

In this paper domain decomposition methods for radiative transfer problems including conductive heat transfer are treated. The paper focuses on semi-transparent materials, like glass, and the associated conditions at the interface between the materials. Using asymptotic analysis we derive conditions for the coupling of the radiative transfer equations and a diffusion approximation. Several test cases are treated and a problem appearing in glass manufacturing processes is computed. The results clearly show the advantages of a domain decomposition approach. Accuracy equivalent to the solution of the global radiative transfer solution is achieved, whereas computation time is strongly reduced.
(24 pages, 1998)

7. I. Choquet

Heterogeneous catalysis modelling and numerical simulation in rarified gas flows Part I: Coverage locally at equilibrium

A new approach is proposed to model and simulate numerically heterogeneous catalysis in rarefied gas flows. It is developed to satisfy all together the following points:
1) describe the gas phase at the microscopic scale, as required in rarefied flows,
2) describe the wall at the macroscopic scale, to avoid prohibitive computational costs and consider not only crystalline but also amorphous surfaces,
3) reproduce on average macroscopic laws correlated with experimental results and
4) derive analytic models in a systematic and exact way. The problem is stated in the general framework of a non static flow in the vicinity of a catalytic and non porous surface (without aging). It is shown that the exact and systematic resolution method based on the Laplace transform, introduced previously by the author to model collisions in the gas phase, can be extended to the present problem. The proposed approach is applied to the modelling of the EleyRideal and LangmuirHinshelwood recombinations, assuming that the coverage is locally at equilibrium. The models are developed considering one atomic species and extended to the general case of several atomic species. Numerical calculations show that the models derived in this way reproduce with accuracy behaviors observed experimentally.
(24 pages, 1998)

8. J. Ohser, B. Steinbach, C. Lang

Efficient Texture Analysis of Binary Images

A new method of determining some characteristics of binary images is proposed based on a special linear filtering. This technique enables the estimation of the area fraction, the specific line length, and the specific integral of curvature. Furthermore, the specific length of the total projection is obtained, which gives detailed information about the texture of the image. The influence of lateral and directional resolution depending on the size of the applied filter mask is discussed in detail. The technique includes a method of increasing directional resolution for texture analysis while keeping lateral resolution as high as possible.
(17 pages, 1998)

9. J. Orlik

Homogenization for viscoelasticity of the integral type with aging and shrinkage

A multiphase composite with periodic distributed inclusions with a smooth boundary is considered in this contribution. The composite component materials are supposed to be linear viscoelastic and aging (of the nonconvolution integral type, for which the Laplace transform with respect to time is not effectively applicable) and are subjected to isotropic shrinkage. The free shrinkage deformation can be considered as a fictitious temperature deformation in the behavior law. The procedure presented in this paper proposes a way to determine average (effective homogenized) viscoelastic and shrinkage (temperature) composite properties and the homogenized stressfield from known properties of the components. This is done by the extension of the asymptotic homogenization technique known for pure elastic nonhomogeneous bodies to the nonhomogeneous thermoviscoelasticity of the integral noncon-

volution type. Up to now, the homogenization theory has not covered viscoelasticity of the integral type. SanchezPalencia (1980), Francfort & Suquet (1987) (see [2], [9]) have considered homogenization for viscoelasticity of the differential form and only up to the first derivative order. The integralmodeled viscoelasticity is more general then the differential one and includes almost all known differential models. The homogenization procedure is based on the construction of an asymptotic solution with respect to a period of the composite structure. This reduces the original problem to some auxiliary boundary value problems of elasticity and viscoelasticity on the unit periodic cell, of the same type as the original non-homogeneous problem. The existence and uniqueness results for such problems were obtained for kernels satisfying some constrain conditions. This is done by the extension of the Volterra integral operator theory to the Volterra operators with respect to the time, whose 1 kernels are space linear operators for any fixed time variables. Some ideas of such approach were proposed in [11] and [12], where the Volterra operators with kernels depending additionally on parameter were considered. This manuscript delivers results of the same nature for the case of the spaceoperator kernels.
(20 pages, 1998)

10. J. Mohring

Helmholtz Resonators with Large Aperture

The lowest resonant frequency of a cavity resonator is usually approximated by the classical Helmholtz formula. However, if the opening is rather large and the front wall is narrow this formula is no longer valid. Here we present a correction which is of third order in the ratio of the diameters of aperture and cavity. In addition to the high accuracy it allows to estimate the damping due to radiation. The result is found by applying the method of matched asymptotic expansions. The correction contains form factors describing the shapes of opening and cavity. They are computed for a number of standard geometries. Results are compared with numerical computations.
(21 pages, 1998)

11. H. W. Hamacher, A. Schöbel

On Center Cycles in Grid Graphs

Finding "good" cycles in graphs is a problem of great interest in graph theory as well as in locational analysis. We show that the center and median problems are NP hard in general graphs. This result holds both for the variable cardinality case (i.e. all cycles of the graph are considered) and the fixed cardinality case (i.e. only cycles with a given cardinality p are feasible). Hence it is of interest to investigate special cases where the problem is solvable in polynomial time. In grid graphs, the variable cardinality case is, for instance, trivially solvable if the shape of the cycle can be chosen freely. If the shape is fixed to be a rectangle one can analyze rectangles in grid graphs with, in sequence, fixed dimension, fixed cardinality, and variable cardinality. In all cases a complete characterization of the optimal cycles and closed form expressions of the optimal objective values are given, yielding polynomial time algorithms for all cases of center rectangle problems. Finally, it is shown that center cycles can be chosen as rectangles for small cardinalities such that the center cycle problem in grid graphs is in these cases completely solved.
(15 pages, 1998)

12. H. W. Hamacher, K.-H. Küfer

Inverse radiation therapy planning - a multiple objective optimisation approach

For some decades radiation therapy has been proved successful in cancer treatment. It is the major task of clinical radiation treatment planning to realize on the one hand a high level dose of radiation in the cancer tissue in order to obtain maximum tumor control. On the other hand it is obvious that it is absolutely necessary to keep in the tissue outside the tumor, particularly in organs at risk, the unavoidable radiation as low as possible.
No doubt, these two objectives of treatment planning - high level dose in the tumor, low radiation outside the tumor - have a basically contradictory nature. Therefore, it is no surprise that inverse mathematical models with dose distribution bounds tend to be infeasible in most cases. Thus, there is need for approximations compromising between overdosing the organs at risk and underdosing the target volume.
Differing from the currently used time consuming iterative approach, which measures deviation from an ideal (non-achievable) treatment plan using recursively trial-and-error weights for the organs of interest, we go a new way trying to avoid a priori weight choices and consider the treatment planning problem as a multiple objective linear programming problem: with each organ of interest, target tissue as well as organs at risk, we associate an objective function measuring the maximal deviation from the prescribed doses.
We build up a data base of relatively few efficient solutions representing and approximating the variety of Pareto solutions of the multiple objective linear programming problem. This data base can be easily scanned by physicians looking for an adequate treatment plan with the aid of an appropriate online tool.
(14 pages, 1999)

13. C. Lang, J. Ohser, R. Hilfer

On the Analysis of Spatial Binary Images

This paper deals with the characterization of microscopically heterogeneous, but macroscopically homogeneous spatial structures. A new method is presented which is strictly based on integral-geometric formulae such as Crofton's intersection formulae and Hadwiger's recursive definition of the Euler number. The corresponding algorithms have clear advantages over other techniques. As an example of application we consider the analysis of spatial digital images produced by means of Computer Assisted Tomography.
(20 pages, 1999)

14. M. Junk

On the Construction of Discrete Equilibrium Distributions for Kinetic Schemes

A general approach to the construction of discrete equilibrium distributions is presented. Such distribution functions can be used to set up Kinetic Schemes as well as Lattice Boltzmann methods. The general principles are also applied to the construction of Chapman Enskog distributions which are used in Kinetic Schemes for compressible Navier-Stokes equations.
(24 pages, 1999)

15. M. Junk, S. V. Raghurame Rao

A new discrete velocity method for Navier-Stokes equations

The relation between the Lattice Boltzmann Method, which has recently become popular, and the Kinetic Schemes, which are routinely used in Computational Fluid Dynamics, is explored. A new discrete velocity model for the numerical solution of Navier-Stokes equations for incompressible fluid flow is presented by combining both the approaches. The new scheme can be interpreted as a pseudo-compressibility method and, for a particular choice of parameters, this interpretation carries over to the Lattice Boltzmann Method.
(20 pages, 1999)

16. H. Neunzert

Mathematics as a Key to Key Technologies

The main part of this paper will consist of examples, how mathematics really helps to solve industrial problems; these examples are taken from our Institute for Industrial Mathematics, from research in the Technomathematics group at my university, but also from ECMI groups and a company called TecMath, which originated 10 years ago from my university group and has already a very successful history.
(39 pages (4 PDF-Files), 1999)

17. J. Ohser, K. Sandau

Considerations about the Estimation of the Size Distribution in Wicksell's Corpuscle Problem

Wicksell's corpuscle problem deals with the estimation of the size distribution of a population of particles, all having the same shape, using a lower dimensional sampling probe. This problem was originary formulated for particle systems occurring in life sciences but its solution is of actual and increasing interest in materials science. From a mathematical point of view, Wicksell's problem is an inverse problem where the interesting size distribution is the unknown part of a Volterra equation. The problem is often regarded ill-posed, because the structure of the integrand implies unstable numerical solutions. The accuracy of the numerical solutions is considered here using the condition number, which allows to compare different numerical methods with different (equidistant) class sizes and which indicates, as one result, that a finite section thickness of the probe reduces the numerical problems. Furthermore, the relative error of estimation is computed which can be split into two parts. One part consists of the relative discretization error that increases for increasing class size, and the second part is related to the relative statistical error which increases with decreasing class size. For both parts, upper bounds can be given and the sum of them indicates an optimal class width depending on some specific constants.
(18 pages, 1999)

18. E. Carrizosa, H. W. Hamacher, R. Klein, S. Nickel

Solving nonconvex planar location problems by finite dominating sets

It is well-known that some of the classical location problems with polyhedral gauges can be solved in polynomial time by finding a finite dominating set, i.e. a finite set of candidates guaranteed to contain at least one optimal location.
In this paper it is first established that this result holds

for a much larger class of problems than currently considered in the literature. The model for which this result can be proven includes, for instance, location problems with attraction and repulsion, and location-allocation problems.
Next, it is shown that the approximation of general gauges by polyhedral ones in the objective function of our general model can be analyzed with regard to the subsequent error in the optimal objective value. For the approximation problem two different approaches are described, the sandwich procedure and the greedy algorithm. Both of these approaches lead - for fixed epsilon - to polynomial approximation algorithms with accuracy epsilon for solving the general model considered in this paper.
Keywords: Continuous Location, Polyhedral Gauges, Finite Dominating Sets, Approximation, Sandwich Algorithm, Greedy Algorithm
(19 pages, 2000)

19. A. Becker

A Review on Image Distortion Measures

Within this paper we review image distortion measures. A distortion measure is a criterion that assigns a "quality number" to an image. We distinguish between mathematical distortion measures and those distortion measures in-cooperating a priori knowledge about the imaging devices (e. g. satellite images), image processing algorithms or the human physiology. We will consider representative examples of different kinds of distortion measures and are going to discuss them.
Keywords: Distortion measure, human visual system
(26 pages, 2000)

20. H. W. Hamacher, M. Labbé, S. Nickel, T. Sonneborn

Polyhedral Properties of the Uncapacitated Multiple Allocation Hub Location Problem

We examine the feasibility polyhedron of the uncapacitated hub location problem (UHL) with multiple allocation, which has applications in the fields of air passenger and cargo transportation, telecommunication and postal delivery services. In particular we determine the dimension and derive some classes of facets of this polyhedron. We develop some general rules about lifting facets from the uncapacitated facility location (UFL) for UHL and projecting facets from UHL to UFL. By applying these rules we get a new class of facets for UHL which dominates the inequalities in the original formulation. Thus we get a new formulation of UHL whose constraints are all facet–defining. We show its superior computational performance by benchmarking it on a well known data set.
Keywords: integer programming, hub location, facility location, valid inequalities, facets, branch and cut
(21 pages, 2000)

21. H. W. Hamacher, A. Schöbel

Design of Zone Tariff Systems in Public Transportation

Given a public transportation system represented by its stops and direct connections between stops, we consider two problems dealing with the prices for the customers: The fare problem in which subsets of stops are already aggregated to zones and "good" tariffs have to be found in the existing zone system. Closed form solutions for the fare problem are presented for three objective functions. In the zone problem the design of the zones is part of the problem. This problem is NP hard and we therefore propose three heuristics which prove to be very successful in the redesign of one of Germany's transportation systems.
(30 pages, 2001)

22. D. Hietel, M. Junk, R. Keck, D. Teleaga:

The Finite-Volume-Particle Method for Conservation Laws

In the Finite-Volume-Particle Method (FVPM), the weak formulation of a hyperbolic conservation law is discretized by restricting it to a discrete set of test functions. In contrast to the usual Finite-Volume approach, the test functions are not taken as characteristic functions of the control volumes in a spatial grid, but are chosen from a partition of unity with smooth and overlapping partition functions (the particles), which can even move along pre- scribed velocity fields. The information exchange between particles is based on standard numerical flux functions. Geometrical information, similar to the surface area of the cell faces in the Finite-Volume Method and the corresponding normal directions are given as integral quantities of the partition functions. After a brief derivation of the Finite-Volume-Particle Method, this work focuses on the role of the geometric coefficients in the scheme.
(16 pages, 2001)

23. T. Bender, H. Hennes, J. Kalcsics, M. T. Melo, S. Nickel

Location Software and Interface with GIS and Supply Chain Management

The objective of this paper is to bridge the gap between location theory and practice. To meet this objective focus is given to the development of software capable of addressing the different needs of a wide group of users. There is a very active community on location theory encompassing many research fields such as operations research, computer science, mathematics, engineering, geography, economics and marketing. As a result, people working on facility location problems have a very diverse background and also different needs regarding the software to solve these problems. For those interested in non-commercial applications (e. g. students and researchers), the library of location algorithms (LoLA can be of considerable assistance. LoLA contains a collection of efficient algorithms for solving planar, network and discrete facility location problems. In this paper, a detailed description of the functionality of LoLA is presented. In the fields of geography and marketing, for instance, solving facility location problems requires using large amounts of demographic data. Hence, members of these groups (e. g. urban planners and sales managers) often work with geographical information too s. To address the specific needs of these users, LoLA was inked to a geographical information system (GIS) and the details of the combined functionality are described in the paper. Finally, there is a wide group of practitioners who need to solve large problems and require special purpose software with a good data interface. Many of such users can be found, for example, in the area of supply chain management (SCM). Logistics activities involved in strategic SCM include, among others, facility location planning. In this paper, the development of a commercial location software tool is also described. The too is embedded in the Advanced Planner and Optimizer SCM software developed by SAP AG, Walldorf, Germany. The paper ends with some conclusions and an outlook to future activities.
Keywords: facility location, software development, geographical information systems, supply chain management.
(48 pages, 2001)

24. H. W. Hamacher, S. A. Tjandra

Mathematical Modelling of Evacuation Problems: A State of Art

This paper details models and algorithms which can be applied to evacuation problems. While it concentrates on building evacuation many of the results are applicable also to regional evacuation. All models consider the time as main parameter, where the travel time between components of the building is part of the input and the overall evacuation time is the output. The paper distinguishes between macroscopic and microscopic evacuation models both of which are able to capture the evacuees' movement over time.
Macroscopic models are mainly used to produce good lower bounds for the evacuation time and do not consider any individual behavior during the emergency situation. These bounds can be used to analyze existing buildings or help in the design phase of planning a building. Macroscopic approaches which are based on dynamic network flow models (minimum cost dynamic flow, maximum dynamic flow, universal maximum flow, quickest path and quickest flow) are described. A special feature of the presented approach is the fact, that travel times of evacuees are not restricted to be constant, but may be density dependent. Using multicriteria optimization priority regions and blockage due to fire or smoke may be considered. It is shown how the modelling can be done using time parameter either as discrete or continuous parameter.
Microscopic models are able to model the individual evacuee's characteristics and the interaction among evacuees which influence their movement. Due to the corresponding huge amount of data one uses simulation approaches. Some probabilistic laws for individual evacuee's movement are presented. Moreover ideas to model the evacuee's movement using cellular automata (CA) and resulting software are presented. In this paper we will focus on macroscopic models and only summarize some of the results of the microscopic approach. While most of the results are applicable to general evacuation situations, we concentrate on building evacuation.
(44 pages, 2001)

25. J. Kuhnert, S. Tiwari

Grid free method for solving the Poisson equation

A Grid free method for solving the Poisson equation is presented. This is an iterative method. The method is based on the weighted least squares approximation in which the Poisson equation is enforced to be satisfied in every iterations. The boundary conditions can also be enforced in the iteration process. This is a local approximation procedure. The Dirichlet, Neumann and mixed boundary value problems on a unit square are presented and the analytical solutions are compared with the exact solutions. Both solutions matched perfectly.
Keywords: Poisson equation, Least squares method, Grid free method
(19 pages, 2001)

26. T. Götz, H. Rave, D. Reinel-Bitzer, K. Steiner, H. Tiemeier

Simulation of the fiber spinning process

To simulate the influence of process parameters to the melt spinning process a fiber model is used and coupled with CFD calculations of the quench air flow. In the fiber model energy, momentum and mass balance are solved for the polymer mass flow. To calculate the quench air the Lattice Boltzmann method is used. Simulations and experiments for different process parameters and hole configurations are compared and show a good agreement.

Keywords: Melt spinning, fiber model, Lattice Boltzmann, CFD

(19 pages, 2001)

27. A. Zemitis

On interaction of a liquid film with an obstacle

In this paper mathematical models for liquid films generated by impinging jets are discussed. Attention is stressed to the interaction of the liquid film with some obstacle. S. G. Taylor [Proc. R. Soc. London Ser. A 253, 313 (1959)] found that the liquid film generated by impinging jets is very sensitive to properties of the wire which was used as an obstacle. The aim of this presentation is to propose a modification of the Taylor's model, which allows to simulate the film shape in cases, when the angle between jets is different from 180°. Numerical results obtained by discussed models give two different shapes of the liquid film similar as in Taylors experiments. These two shapes depend on the regime: either droplets are produced close to the obstacle or not. The difference between two regimes becomes larger if the angle between jets decreases. Existence of such two regimes can be very essential for some applications of impinging jets, if the generated liquid film can have a contact with obstacles.

Keywords: impinging jets, liquid film, models, numerical solution, shape

(22 pages, 2001)

28. I. Ginzburg, K. Steiner

Free surface lattice-Boltzmann method to model the filling of expanding cavities by Bingham Fluids

The filling process of viscoplastic metal alloys and plastics in expanding cavities is modelled using the lattice Boltzmann method in two and three dimensions. These models combine the regularized Bingham model for viscoplastic with a free-interface algorithm. The latter is based on a modified immiscible lattice Boltzmann model in which one species is the fluid and the other one is considered as vacuum. The boundary conditions at the curved liquid-vacuum interface are met without any geometrical front reconstruction from a first-order Chapman-Enskog expansion. The numerical results obtained with these models are found in good agreement with available theoretical and numerical analysis.

Keywords: Generalized LBE, free-surface phenomena, interface boundary conditions, filling processes, Bingham viscoplastic model, regularized models

(22 pages, 2001)

29. H. Neunzert

»Denn nichts ist für den Menschen als Menschen etwas wert, was er nicht mit Leidenschaft tun kann«

Vortrag anlässlich der Verleihung des Akademiepreises des Landes Rheinland-Pfalz am 21.11.2001

Was macht einen guten Hochschullehrer aus? Auf diese Frage gibt es sicher viele verschiedene, fachbezogene Antworten, aber auch ein paar allgemeine Gesichtspunkte: es bedarf der »Leidenschaft« für die Forschung (Max Weber), aus der dann auch die Begeisterung für die Lehre erwächst. Forschung und Lehre gehören zusammen, um die Wissenschaft als lebendiges Tun vermitteln zu können. Der Vortrag gibt Beispiele dafür, wie in angewandter Mathematik Forschungsaufgaben aus praktischen Alltagsproblemstellungen erwachsen, die in die Lehre auf verschiedenen Stufen (Gymnasium bis Graduiertenkolleg) einfließen; er leitet damit auch zu einem aktuellen Forschungsgebiet, der Mehrskalenanalyse mit ihren vielfältigen Anwendungen in Bildverarbeitung, Materialentwicklung und Strömungsmechanik über, was aber nur kurz gestreift wird. Mathematik erscheint hier als eine moderne Schlüsseltechnologie, die aber auch enge Beziehungen zu den Geistes- und Sozialwissenschaften hat.

Keywords: Lehre, Forschung, angewandte Mathematik, Mehrskalenanalyse, Strömungsmechanik

(18 pages, 2001)

30. J. Kuhnert, S. Tiwari

Finite pointset method based on the projection method for simulations of the incompressible Navier-Stokes equations

A Lagrangian particle scheme is applied to the projection method for the incompressible Navier-Stokes equations. The approximation of spatial derivatives is obtained by the weighted least squares method. The pressure Poisson equation is solved by a local iterative procedure with the help of the least squares method. Numerical tests are performed for two dimensional cases. The Couette flow, Poiseuelle flow, decaying shear flow and the driven cavity flow are presented. The numerical solutions are obtained for stationary as well as instationary cases and are compared with the analytical solutions for channel flows. Finally, the driven cavity in a unit square is considered and the stationary solution obtained from this scheme is compared with that from the finite element method.

Keywords: Incompressible Navier-Stokes equations, Meshfree method, Projection method, Particle scheme, Least squares approximation

AMS subject classification: 76D05, 76M28

(25 pages, 2001)

31. R. Korn, M. Krekel

Optimal Portfolios with Fixed Consumption or Income Streams

We consider some portfolio optimisation problems where either the investor has a desire for an a priori specified consumption stream or/and follows a deterministic pay in scheme while also trying to maximize expected utility from final wealth. We derive explicit closed form solutions for continuous and discrete monetary streams. The mathematical method used is classical stochastic control theory.

Keywords: Portfolio optimisation, stochastic control, HJB equation, discretisation of control problems.

(23 pages, 2002)

32. M. Krekel

Optimal portfolios with a loan dependent credit spread

If an investor borrows money he generally has to pay higher interest rates than he would have received, if he had put his funds on a savings account. The classical model of continuous time portfolio optimisation ignores this effect. Since there is obviously a connection between the default probability and the total percentage of wealth, which the investor is in debt, we study portfolio optimisation with a control dependent interest rate. Assuming a logarithmic and a power utility function, respectively, we prove explicit formulae of the optimal control.

Keywords: Portfolio optimisation, stochastic control, HJB equation, credit spread, log utility, power utility, non-linear wealth dynamics

(25 pages, 2002)

33. J. Ohser, W. Nagel, K. Schladitz

The Euler number of discretized sets - on the choice of adjacency in homogeneous lattices

Two approaches for determining the Euler-Poincaré characteristic of a set observed on lattice points are considered in the context of image analysis { the integral geometric and the polyhedral approach. Information about the set is assumed to be available on lattice points only. In order to retain properties of the Euler number and to provide a good approximation of the true Euler number of the original set in the Euclidean space, the appropriate choice of adjacency in the lattice for the set and its background is crucial. Adjacencies are defined using tessellations of the whole space into polyhedrons. In R 3 , two new 14 adjacencies are introduced additionally to the well known 6 and 26 adjacencies. For the Euler number of a set and its complement, a consistency relation holds. Each of the pairs of adjacencies (14:1; 14:1), (14:2; 14:2), (6; 26), and (26; 6) is shown to be a pair of complementary adjacencies with respect to this relation. That is, the approximations of the Euler numbers are consistent if the set and its background (complement) are equipped with this pair of adjacencies. Furthermore, sufficient conditions for the correctness of the approximations of the Euler number are given. The analysis of selected microstructures and a simulation study illustrate how the estimated Euler number depends on the chosen adjacency. It also shows that there is not a uniquely best pair of adjacencies with respect to the estimation of the Euler number of a set in Euclidean space.

Keywords: image analysis, Euler number, neighborhod relationships, cuboidal lattice

(32 pages, 2002)

34. I. Ginzburg, K. Steiner

Lattice Boltzmann Model for Free-Surface flow and Its Application to Filling Process in Casting

A generalized lattice Boltzmann model to simulate free-surface is constructed in both two and three dimensions. The proposed model satisfies the interfacial boundary conditions accurately. A distinctive feature of the model is that the collision processes is carried out only on the points occupied partially or fully by the fluid. To maintain a sharp interfacial front, the method includes an anti-diffusion algorithm. The unknown distribution functions at the interfacial region are constructed according to the first order Chapman-Enskog analysis. The interfacial boundary conditions are satis-

fied exactly by the coefficients in the Chapman-Enskog expansion. The distribution functions are naturally expressed in the local interfacial coordinates. The macroscopic quantities at the interface are extracted from the least-square solutions of a locally linearized system obtained from the known distribution functions. The proposed method does not require any geometric front construction and is robust for any interfacial topology. Simulation results of realistic filling process are presented: rectangular cavity in two dimensions and Hammer box, Campbell box, Sheffield box, and Motorblock in three dimensions. To enhance the stability at high Reynolds numbers, various upwind-type schemes are developed. Free-slip and no-slip boundary conditions are also discussed.
Keywords: Lattice Boltzmann models; free-surface phenomena; interface boundary conditions; filling processes; injection molding; volume of fluid method; interface boundary conditions; advection-schemes; upwind-schemes
(54 pages, 2002)

35. M. Günther, A. Klar, T. Materne, R. Wegener

Multivalued fundamental diagrams and stop and go waves for continuum traffic equations

In the present paper a kinetic model for vehicular traffic leading to multivalued fundamental diagrams is developed and investigated in detail. For this model phase transitions can appear depending on the local density and velocity of the flow. A derivation of associated macroscopic traffic equations from the kinetic equation is given. Moreover, numerical experiments show the appearance of stop and go waves for highway traffic with a bottleneck.
Keywords: traffic flow, macroscopic equations, kinetic derivation, multivalued fundamental diagram, stop and go waves, phase transitions
(25 pages, 2002)

36. S. Feldmann, P. Lang, D. Prätzel-Wolters

Parameter influence on the zeros of network determinants

To a network N(q) with determinant D(s;q) depending on a parameter vector $q \hat{I} R^r$ via identification of some of its vertices, a network N^ (q) is assigned. The paper deals with procedures to find N^ (q), such that its determinant D^ (s;q) admits a factorization in the determinants of appropriate subnetworks, and with the estimation of the deviation of the zeros of D^ from the zeros of D. To solve the estimation problem state space methods are applied.
Keywords: Networks, Equicofactor matrix polynomials, Realization theory, Matrix perturbation theory
(30 pages, 2002)

37. K. Koch, J. Ohser, K. Schladitz

Spectral theory for random closed sets and estimating the covariance via frequency space

A spectral theory for stationary random closed sets is developed and provided with a sound mathematical basis. Definition and proof of existence of the Bartlett spectrum of a stationary random closed set as well as the proof of a Wiener-Khintchine theorem for the power spectrum are used to two ends: First, well known second order characteristics like the covariance can be estimated faster than usual via frequency space. Second, the Bartlett spectrum and the power spectrum can be used as second order characteristics in frequency space. Examples show, that in some cases information about the random closed set is easier to obtain from these characteristics in frequency space than from their real world counterparts.
Keywords: Random set, Bartlett spectrum, fast Fourier transform, power spectrum
(28 pages, 2002)

38. D. d'Humières, I. Ginzburg

Multi-reflection boundary conditions for lattice Boltzmann models

We present a unified approach of several boundary conditions for lattice Boltzmann models. Its general framework is a generalization of previously introduced schemes such as the bounce-back rule, linear or quadratic interpolations, etc. The objectives are two fold: first to give theoretical tools to study the existing boundary conditions and their corresponding accuracy; secondly to design formally third- order accurate boundary conditions for general flows. Using these boundary conditions, Couette and Poiseuille flows are exact solution of the lattice Boltzmann models for a Reynolds number $Re = 0$ (Stokes limit).
Numerical comparisons are given for Stokes flows in periodic arrays of spheres and cylinders, linear periodic array of cylinders between moving plates and for Navier-Stokes flows in periodic arrays of cylinders for $Re < 200$. These results show a significant improvement of the overall accuracy when using the linear interpolations instead of the bounce-back reflection (up to an order of magnitude on the hydrodynamics fields). Further improvement is achieved with the new multi-reflection boundary conditions, reaching a level of accuracy close to the quasi-analytical reference solutions, even for rather modest grid resolutions and few points in the narrowest channels. More important, the pressure and velocity fields in the vicinity of the obstacles are much smoother with multi-reflection than with the other boundary conditions.
Finally the good stability of these schemes is highlighted by some simulations of moving obstacles: a cylinder between flat walls and a sphere in a cylinder.
Keywords: lattice Boltzmann equation, boudary condistions, bounce-back rule, Navier-Stokes equation
(72 pages, 2002)

39. R. Korn

Elementare Finanzmathematik

Im Rahmen dieser Arbeit soll eine elementar gehaltene Einführung in die Aufgabenstellungen und Prinzipien der modernen Finanzmathematik gegeben werden. Insbesondere werden die Grundlagen der Modellierung von Aktienkursen, der Bewertung von Optionen und der Portfolio-Optimierung vorgestellt. Natürlich können die verwendeten Methoden und die entwickelte Theorie nicht in voller Allgemeinheit für den Schulunterricht verwendet werden, doch sollen einzelne Prinzipien so heraus gearbeitet werden, dass sie auch an einfachen Beispielen verstanden werden können.
Keywords: Finanzmathematik, Aktien, Optionen, Portfolio-Optimierung, Börse, Lehrerweiterbildung, Mathematikunterricht
(98 pages, 2002)

40. J. Kallrath, M. C. Müller, S. Nickel

Batch Presorting Problems: Models and Complexity Results

In this paper we consider short term storage systems. We analyze presorting strategies to improve the effiency of these storage systems. The presorting task is called Batch PreSorting Problem (BPSP). The BPSP is a variation of an assigment problem, i. e., it has an assigment problem kernel and some additional constraints. We present different types of these presorting problems, introduce mathematical programming formulations and prove the NP-completeness for one type of the BPSP. Experiments are carried out in order to compare the different model formulations and to investigate the behavior of these models.
Keywords: Complexity theory, Integer programming, Assigment, Logistics
(19 pages, 2002)

41. J. Linn

On the frame-invariant description of the phase space of the Folgar-Tucker equation

The Folgar-Tucker equation is used in flow simulations of fiber suspensions to predict fiber orientation depending on the local flow. In this paper, a complete, frame-invariant description of the phase space of this differential equation is presented for the first time.
Key words: fiber orientation, Folgar-Tucker equation, injection molding
(5 pages, 2003)

42. T. Hanne, S. Nickel

A Multi-Objective Evolutionary Algorithm for Scheduling and Inspection Planning in Software Development Projects

In this article, we consider the problem of planning inspections and other tasks within a software development (SD) project with respect to the objectives quality (no. of defects), project duration, and costs. Based on a discrete-event simulation model of SD processes comprising the phases coding, inspection, test, and rework, we present a simplified formulation of the problem as a multiobjective optimization problem. For solving the problem (i. e. finding an approximation of the efficient set) we develop a multiobjective evolutionary algorithm. Details of the algorithm are discussed as well as results of its application to sample problems.
Key words: multiple objective programming, project management and scheduling, software development, evolutionary algorithms, efficient set
(29 pages, 2003)

43. T. Bortfeld , K.-H. Küfer, M. Monz, A. Scherrer, C. Thieke, H. Trinkaus

Intensity-Modulated Radiotherapy - A Large Scale Multi-Criteria Programming Problem -

Radiation therapy planning is always a tight rope walk between dangerous insufficient dose in the target volume and life threatening overdosing of organs at risk. Finding ideal balances between these inherently contradictory goals challenges dosimetrists and physicians in their daily practice. Today's planning systems are typically based on a single evaluation function that measures the quality of a radiation treatment plan. Unfortunately, such a one dimensional approach can-

not satisfactorily map the different backgrounds of physicians and the patient dependent necessities. So, too often a time consuming iteration process between evaluation of dose distribution and redefinition of the evaluation function is needed.
In this paper we propose a generic multi-criteria approach based on Pareto's solution concept. For each entity of interest - target volume or organ at risk a structure dependent evaluation function is defined measuring deviations from ideal doses that are calculated from statistical functions. A reasonable bunch of clinically meaningful Pareto optimal solutions are stored in a data base, which can be interactively searched by physicians. The system guarantees dynamical planning as well as the discussion of tradeoffs between different entities.
Mathematically, we model the upcoming inverse problem as a multi-criteria linear programming problem. Because of the large scale nature of the problem it is not possible to solve the problem in a 3D-setting without adaptive reduction by appropriate approximation schemes.
Our approach is twofold: First, the discretization of the continuous problem is based on an adaptive hierarchical clustering process which is used for a local refinement of constraints during the optimization procedure. Second, the set of Pareto optimal solutions is approximated by an adaptive grid of representatives that are found by a hybrid process of calculating extreme compromises and interpolation methods.
Keywords: multiple criteria optimization, representative systems of Pareto solutions, adaptive triangulation, clustering and disaggregation techniques, visualization of Pareto solutions, medical physics, external beam radiotherapy planning, intensity modulated radiotherapy
(31 pages, 2003)

Status quo: January 2003